PERFORMANCE ANALYSIS OF GEOTHERMAL TURBINE SET FOR WELL-HEAD POWER PLANTS: CASE STUDY OF OLKARIA, KENYA

BY

RUTO HILLARY KIPRONO

Thesis submitted to the School of Engineering, Department of Mechanical & Production Engineering in partial fulfillment for the requirements of the award of the Degree of

MASTER OF SCIENCE

In

ENERGY STUDIES

MOI UNIVERSITY

2021

DECLARATION

Declaration by Candidate:

I declare that this thesis is my original work and has not been submitted for a degree in any other university or educational institution. No part of this thesis may be reproduced in any form without the prior permission of the author and/or Moi University.

Signature:_____ Date:_____

Ruto Hillary Kiprono

TEC/PGMP/18/18

Declaration by Supervisors

We declare that this thesis has been submitted for examination with our approval as university supervisors.

Signature:_____ Date:_____

Prof. Zachary Otara Siagi,
Dept. of Mechanical & Production Eng.,
School of Engineering,
Moi University.

Signature:_____ Date:_____

Prof. Josphat Igadwa Mwasiagi,
Dept. of Manufacturing, Industrial & Textile Eng.,
School of Engineering,
Moi University.

DEDICATION

I dedicate this research thesis to my parents Mr. and Mrs. David Koech, my dear wife Mrs Lucy Chepkoech, my sons Arnold and Adrian, my brother Kevin and to my sisters; Vicky, Aneth and Faith.

ACKNOWLEDGEMENT

I would like to extend my gratitude and to acknowledge the following key people who supported this work by contributing generously and tirelessly to the success of the work presented in this research thesis.

My Supervisors, Prof. Zachary Otara Siagi and Prof. Josphat Igadwa Mwasiagi, for their valuable support and guidance throughout the entire course of this research. ACE II PTRE and Moi University staff for their unconditional support during my tenure in the institution. To my Projects Director Mr. Puneet Shamshery and Mr. Kishor Pindolia. Similar gratitude to my colleagues Mohammed, Chida, Alex, Malanda, Mwape, Zeddy and all my classmates.

To the following institutions for their financial, technical and expert support that made this research a success. Ministry of Education (Project No: MOE/HEST/04/2017-2018), ACE-II PTRE center, African Development Bank (AFDB), Moi University, and Kenya Electricity Generating Company (Kengen).

To my family members for your unconditional love, prayers, patience and for an exceptional moral support that uplifted my spirit to move on even during tough times without giving up.

Finally, and above all, to the Almighty God for His grace, good health and unending Love.

ABSTRACT

Globally, geothermal energy utilization for power generation has been ongoing for decades through conventional technologies. In 2012, Well-head technology was first utilized in Kenya's Olkaria geothermal field. However, severe cases of erosion/corrosion and deposition/scaling were observed within the turbine set after hardly five years of operation. These defects greatly impacted on the plant's performance by reducing its energy conversion efficiency and output. The main objective of this research was to investigate the factors affecting the performance of the turbines at Olkaria's well-head power plants. Its specific objectives were to determine the composition of geothermal fluid, characterize the solid deposits in comparison with the turbine blade material, determine the causes of observed defects, determine the methods of eliminating the defects and to enhance performance of the turbines by implementing selected methods of eliminating the defects at Olkaria's well-head power plants. Analyses of geothermal fluids at various sections of the plant were done using the potentiometric, AAS and spectrophotometric techniques to determine its composition. Analyses of solid deposits were done using XRD and XRF techniques. Blade sample analysis was done using Metal scan spectroscopy and XRF techniques. Literature review guided an inferential approach used to determine the causes of the defects. Manufacturing & maintenance standards were used to determine methods of eliminating the defects. The characteristics of geothermal fluid entering the turbine were found to be; pH (4.55), TDS (12.40 ppt), Conductivity (24.78 µs/cm), chloride ions (6.59 ppm), Sulphate ions (6.27 ppm), silica (2.71 ppm), Iron (1.56 mg/L) and Sodium (1.03 mg/L). The solid deposits on the turbine consisted of silica in form of SiO_2 (66.20%) iron, Fe (13.78%), K_2O (9.08%), Sulphur (3.40%), chlorides (2.48%), P_2O_5(1.69%), Calcium (1.23%), Barium (0.7%), Manganese (0.62%), titanium (0.39%), and Chromium (0.19%).The turbine blade material was characterized as an alloy steel with the highest composition being iron (Fe 82.64%), and an average chromium content of 12.50%. The pH value, chloride and sulphate ions in the fluid signify acidity and its highly corrosive nature. Significant amounts of oxides in deposits indicate oxidation reactions as the fluid interacts with the metals at elevated temperatures leading to deposition/scaling. As observed, the turbine blade was highly affected by corrosion. This was attributed to the parent material, 12.5%Cr steel alloy, having low resistance to corrosion under the operating conditions of the turbine. In conclusion, the results attributed the root cause of the defects to steam quality and blade material resistance to corrosion. Based on this conclusion, hard facing and machining techniques were determined as suitable methods of eliminating the defects. These methods were implemented to refurbish an affected turbine and in the process, a material composed of 23.9%Cr, 13.0% Ni, 1.8%Mn and 0.15%Mo (AWS A5.9:ER309L) was selected as a suitable overlay material for the repair in view of its fusion characteristics, toughness, tensile and creep strengths. The refurbishment resulted in improving the turbine's output from 2.75 MW to its design rated output of 3.20 MW. Considering the same quantity of steam being consumed, the energy conversion efficiency was increased by 16.4%; hence, the turbine performance was enhanced. However, further research was recommended to investigate the impacts of hard facing and machining techniques on the life span of the turbine.

TABLE OF CONTENTS

LIST OF TABLES

LIST OF FIGURES

LIST OF PLATES

ACRONYMS AND ABBREVIATIONS

C:	Carbon
Cr:	Chromium
HAZ:	Heat Affected Zone
HP:	High Pressure
HVOF:	High Velocity Oxygen Fuel
H_2S:	Hydrogen Sulphide
KenGen:	Kenya Electricity Generating Company Ltd
KWG:	KenGen Wellhead Generator
LP:	Low Pressure
Mn:	Manganese
Mo:	Molybdenum
MPa:	Mega Pascals
MW:	Mega Watt
NCG:	Non-Condensable Gases
Ni:	Nickel
OEM:	Original Equipment Manufacturer
OLK:	Olkaria
pH	Potential hydrogen
R&D	Research and Development
RPM	Revolutions per minute
SCC	Stress Corrosion Cracking
Si:	Silica

CHAPTER ONE

INTRODUCTION

1.1 Background Information

Geothermal energy contributes a tiny proportion of the world's primary energy consumption. In electricity generation, geothermal produces less than 1% of the world's output. However, individual countries which lack indigenous fossil fuels, geothermal energy contributes materially to the nation's energy supply. In the recent past, Turkey accounted for half of the new global capacity additions, followed by the United States, Mexico, Kenya, Japan and Germany as illustrated in figure 1.1 (GEA report, 2016).

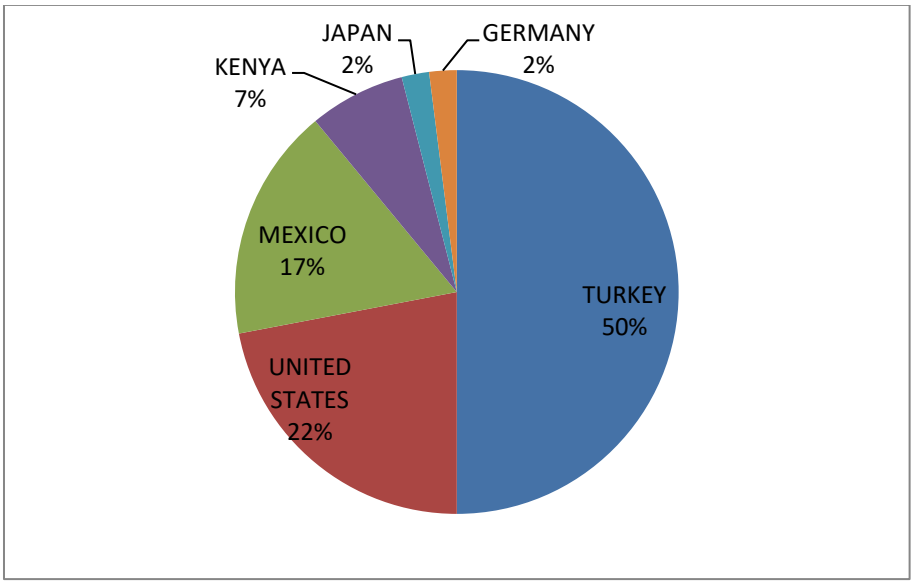

Figure 1. 1: New Global Geothermal Capacity Additions
Source: Geothermal Energy Association (GEA) report (2016)

In Kenya, various sources of energy have been utilized to generate electricity ranging from hydro, geothermal, thermal and wind. Currently, the national electricity generation by mode is 47% geothermal, 39% hydro, 13% thermal and 1% wind (Kengen, 2016). This indicates that geothermal energy is the major source of power in the country. With the global shift towards clean, environmentally friendly renewable

energy, exploration and infrastructure development in geothermal power is actively pursued.

1.2 Problem Environment

Geothermal power generation technology extracts a mixture of steam and brine that has been heated by geothermal heat from a production well approximately 3000 metres deep, and uses that energy to drive a turbine coupled to a generator used to generate electricity. Since there is no need to burn fuels such as oil, coal and natural gas, there is almost no emission of such environmental pollutants. Geothermal energy is reusable clean energy, and its usage is expected to increase in the future to help prevent global warming.

However, depending on the geological composition and hydrological status of the earth's crust, geothermal steam sometimes contains considerable concentrations of minerals and gases in different volumes consequently affecting its thermodynamic properties. These impurities also contribute to various defects such as erosion/corrosion and scaling/deposition in wells and surface installations within which the geothermal fluids flow.

Large scale geothermal utilization has been ongoing for several decades in the country. Olkaria's geothermal well head power plant was first constructed in the year 2010. The first turbine C50 type was successfully commissioned in the year 2012. The well head technology was the first ever to be developed in the world. However, the development has not been without problems. Ideally, the plants were designed to operate for about 25 years after which they were to be evaluated based on the technical performance and its condition. During the design stages, various factors must have been considered but the recent state observed on the equipment indicated serious defects.

During an annual review on the well head plants' power output for the year 2018, it was realized that one of the units (KWG4 – unit 1) had a constant reduced output from its rated output of 3.2 MW to as low as 2.75MW (Kengen Reports, 2019). This prompted a scheduled inspection of the unit whereby, it was found that it had suffered a severe case of erosion corrosion. The base of the welds enjoining fixed vanes to diaphragm rings had eroded on the inner and outer circumferential joints as shown in figure 1.2. This condition had affected all the seven diaphragms as shown in figure 1.3 and as a result, the fixed vanes had drifted out of position interfering with its operating clearances; hence were scrubbing against the rotor shrouds on the 1st, 3rd and 7th stages as illustrated in figure 1.4.

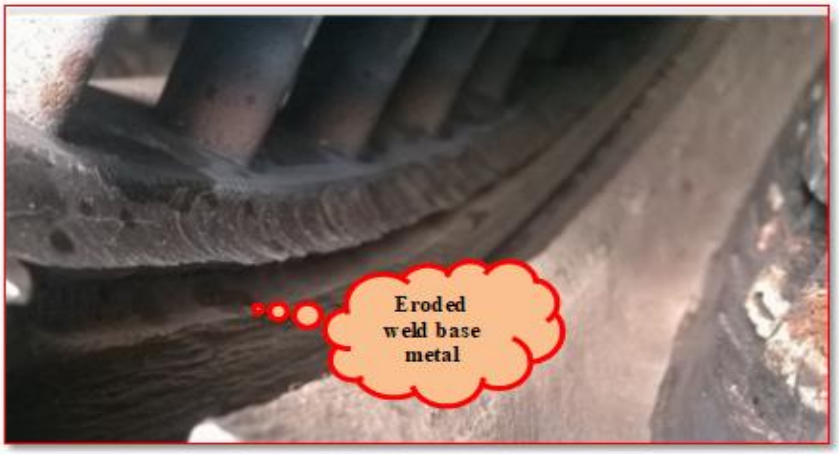

Figure 1.2: Eroded diaphragm base
(Source: Researcher, 2019)

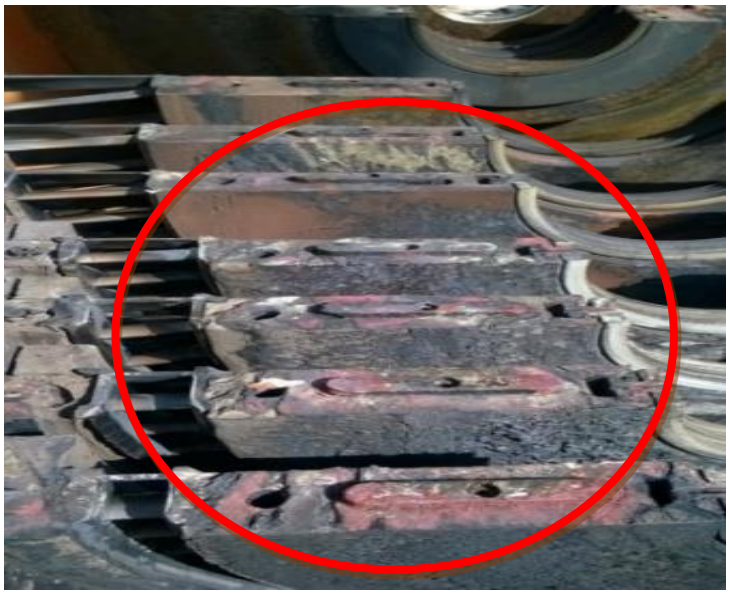

Figure 1.3: Eroded and steam gouged diaphragms
(Source: Researcher, 2019)

Figure 1.4: Scrubbing on rotor
(Source: Researcher, 2019)

Plate 1.1 shows the worn out, stage 1 rotor blades due to corrosion. This causes mass imbalance which consequently leads to vibration during operation. Vibration can then lead to equipment damage and failure.

Plate 1.1: Corrosion on stage 1 Rotor blade

(Source: Researcher, 2019)

Plate 1.2 and 1.3 illustrate corrosion on the rotor blades and diapgram blades, which causes mass reduction resulting in rotor-diaphram clearence variations affecting the steam dynamics inside the steam chamber, and reduces the lifespan of the rotor. Corrosion is caused by the presence of moisture and oxygen. The turbine efficiency drops due to deviation from isentropic behavior and the presence of moisture in the turbine during the steam expansion process (Dipippo, 2008).

Plate 1. 2: corrosion on rotor

Source: Researcher, 2019)

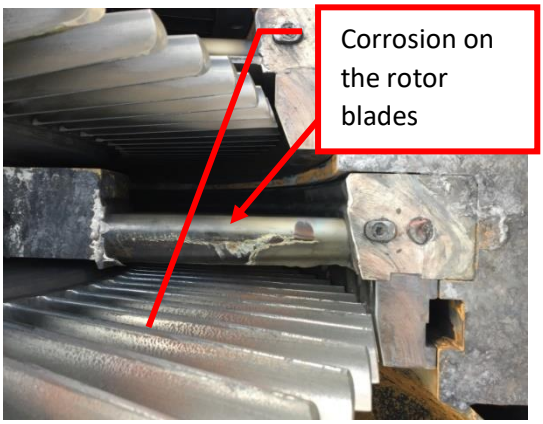

Plate 1. 3: Corrosion on rotor and diaphragm blades

(Source: Researcher, 2019)

Corrosion can result in crevices which can act as impurity traps and facilitate formation of oxygen concentration cells and may generate high stresses by the oxides growth mechanism. The worst crevices are those with corrosive impurities and metal temperature within the salt zone (Ryzekov, 2000).

Plate 1.4 and 1.5 indicate deposition on rotor stage 2 and 3. Deposition causes mass increase, which result in weight imbalances leading to vibration. It also reduces steam passages creating back pressure which results in reduced turbine efficiency. The reduction in turbine power output is as a result of the pressure and flowrate of the working medium dropping due to deposits forming. Components of the steam collection and preparation systems in the turbine set are destroyed, the vacuum becomes degraded as a result of condenser tubes being clogged and damaged also leading to reduced efficiency.

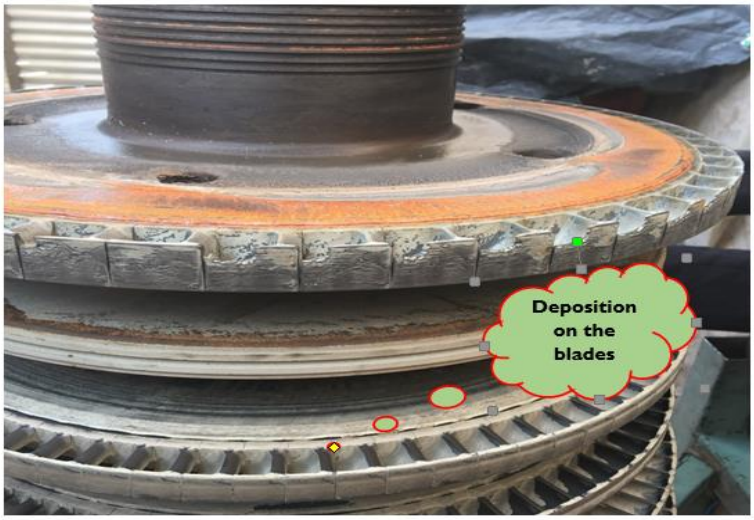

Plate 1. 4: Deposition on the rotor stage 2 and 3

(Source: Researcher, 2019)

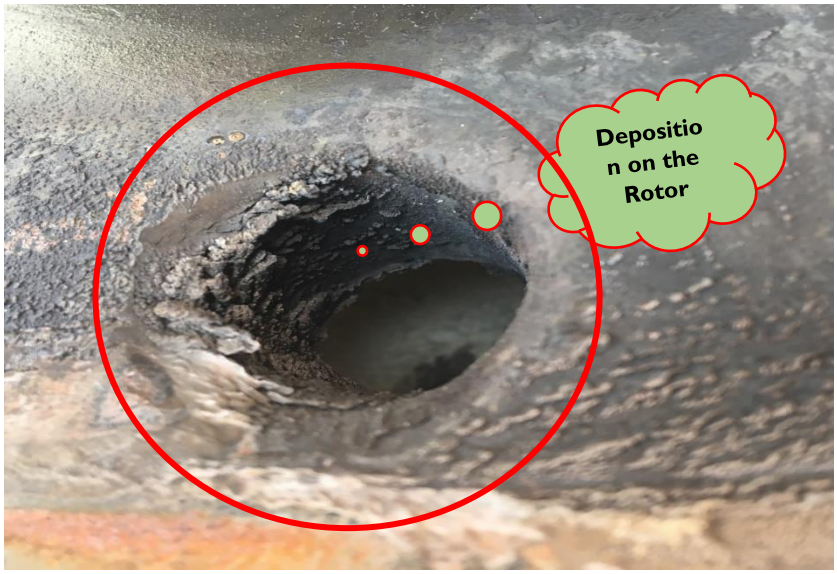

Plate 1. 5: Deposition on rotor

(Source: Researcher, 2019)

This disrepair was untenable and infringing on rotor operating clearances. Based on the location and nature of erosion found in the turbine's diaphragms, it was inferred that the unit suffered more from wet steam erosion than it did from solid particulate matter.

It was therefore inevitably necessary to repair the affected parts of the turbine prior to restarting the unit.

1.3 Problem Statement

The well head technology has been in operation at Olkaria - Kenya for less than 5 years yet the erosion/corrosion and scaling/deposition on the equipment is severe. These defects have greatly impacted on the power plants' performance by reducing its energy conversion efficiency and output.

1.4 Objectives

1.4.1 Main objective

The main objective of the study was to investigate the causes of defects affecting the performance of turbines at Olkaria's well-head power plants.

1.4.2 Specific objectives

i. To determine the composition of geothermal fluid at Olkaria's well-head power plants

ii. To characterize the solid deposits in comparison with the turbine blade material for Olkaria's well-head power plants

iii. To determine the causes of scaling/deposition and corrosion/erosion on turbines at Olkaria's well-head power plants

iv. To determine the methods of eliminating the defects on turbines at Olkaria's well-head power plants

v. To enhance performance of the turbines by implementing selected methods of eliminating the defects at Olkaria's well-head power plants

1.5 Justification

Currently there are 18 seven stage condensing turbines successfully commissioned contributing to 75 MW of electricity to the national grid. This implies that a huge amount of investment have been channeled towards this as geothermal energy development is capital intensive. The technology has also proven to be attractive as the development process is much faster and relatively cheaper as compared to the conventional large scale geothermal power plants.

On the other hand, despite its attractiveness, the technology has a number of challenges. Recently observed cases of erosion/corrosion and scaling/deposition are severe and pose a serious problem owing to the plant performance. Scaling/deposition increase the surface roughness on the steam path leading to increase frictional losses and pressure drop. It also causes increased turbulent flow and in more severe cases, it causes chocking of the steam path leading to back pressure. Erosion/corrosion causes internal leakages that generate turbulent flows and drag forces resulting in pressure loss. Both erosion/corrosion and scaling/deposition causes imbalance as they contribute to uneven mass distribution on the rotating parts of the turbine leading to increased vibrations. Considering that turbines are sensitive high precision equipment, these conditions are highly unfavourable as they reduce the energy conversion efficiency of the plant resulting in reduced plant output. Therefore, there is an urgent need to understand the root cause of the defects (erosion/corrosion and scaling/deposition) on turbines so that proper solutions are determined and implemented to improve on the plants' condition.

CHAPTER TWO

LITERATURE REVIEW

2.1 Background on Geothermal Fluids

The composition of geothermal fluid as it exists naturally in the reservoir ranges from steam in vapor state, hot water in liquid state, Non-Condensable Gases (NCGs) (CO_2, H_2S, NH_3, N_2, CH_4, etc.), solid particles to chemical compounds depending on the geological and hydrological status of the earth's crust. All these components flow out of the production well but the solid particles and liquid water are separated from the rest using a separator. The rest flows through the entire cycle of the geothermal power plants to generate electricity. The presence of corrosive NCGs, require a more corrosion resistant turbine and condenser design. The NCGs in geothermal steam interfere with heat transfer in the condenser by forming a 'gas-blanketing' effect, which raises the condenser temperature and back-pressure on the turbine, reducing its output (Vorum & Fritzler, 2000).

Problems associated with elevated levels of NCGs in geothermal power plants are as follows:

- The gases reduce the heat transfer efficiency of the condensers increasing the condenser operating pressure, which reduces turbine power output, NCGs contain lower recoverable specific energy than steam,
- Higher capital and operating cost for gas removal in the cost of electricity than fossil-fueled power plants,
- Acid gases such as carbon dioxide and hydrogen sulphide are highly water-soluble and contribute to corrosion problems in piping and equipment that contact steam and condensate (Vorum & Fritzler, 2000).

In practice, the gases' effect can only be overcome by evacuating them, along with a portion of steam. Gas removal system is costly in geothermal systems because of elevated gas levels. The power needed to extract the NCGs from the condensers and exhaust them to the atmosphere or an abatement system is supplied from the generated electricity; this seriously impairs the power generation performance (Duthie & Nawaz, 1989). NCGs also decrease the exergy of the fluid reducing the available work in the plant. Thus, evaluation of the network of the turbine should consider the NCG content (Montero, 1990). The influence of NCGs on the performance of geothermal power plants is of significant concern. Presence of 10% NCG in the geothermal steam, results in as much as a 25% decrease in the net-work output compared to a clean steam system (Khalifa & Michaelides, 1978).

Specific chemistry of geothermal steam include high non-condensable gas contents, high content of solids salts dissolved in steam and corrosive chemical composition (Regenspurg, 2010). The steam impurities could be easily transferred to the metal surface and in the process may generate greater concentration of corrosive impurities such as massive amounts of silicide's and salts' deposits. Aggressive/Accelerated corrosion in geothermal steam condition results from the presence of many salt contaminants such as Na_2SO_4, NaCl, and silicates. These contaminants have a damaging impact on the protective surface of geothermal plant components (Cuevas-Artega *et al.,* 2014). For example, high H_2S content generally promotes metallurgical problem such as stress corrosion cracking and metal fatigue (Stefansson, 2014). The high CO_2 content in geothermal fluid 200^oC, accelerate calcite scaling and promote active corrosion. The most common problems regarding high gas content in the geothermal steam are high non-condensable gas contents, Sulphur deposition, corrosion

due to low pH and high oxygen concentrations with moisture in the geothermal power components and in the steam itself (Ahned & Sürken, 2009).

2.2 Characteristics of Olkaria Geothermal Fluids

The geology of the greater Olkaria volcanic complex and the surface outcrops are mainly cemented lavas and their pyroclastic equivalents, ashes from Suswa and Longonot volcanoes with minor trachyte and basalts. Well lithological logs indicate the presence of a basalt (Olkaria basalt) underling the Upper Olkaria volcanos in the Eastern part of the geothermal field. The subsurface geology of the Olkaria Geothermal Field has been classified into six broad lithostratigraphic groups based on age, tectono-stratigraphy, and lithology. The formations in chrono-stratigraphy order from the oldest to the youngest include the Proterozoic "basement" formations, pre-Mau volcanos, Mau Tuffs, Plateau Trachyte, Olkaria Basalts and Upper Olkaria Volcanos (Omenda, 2000).

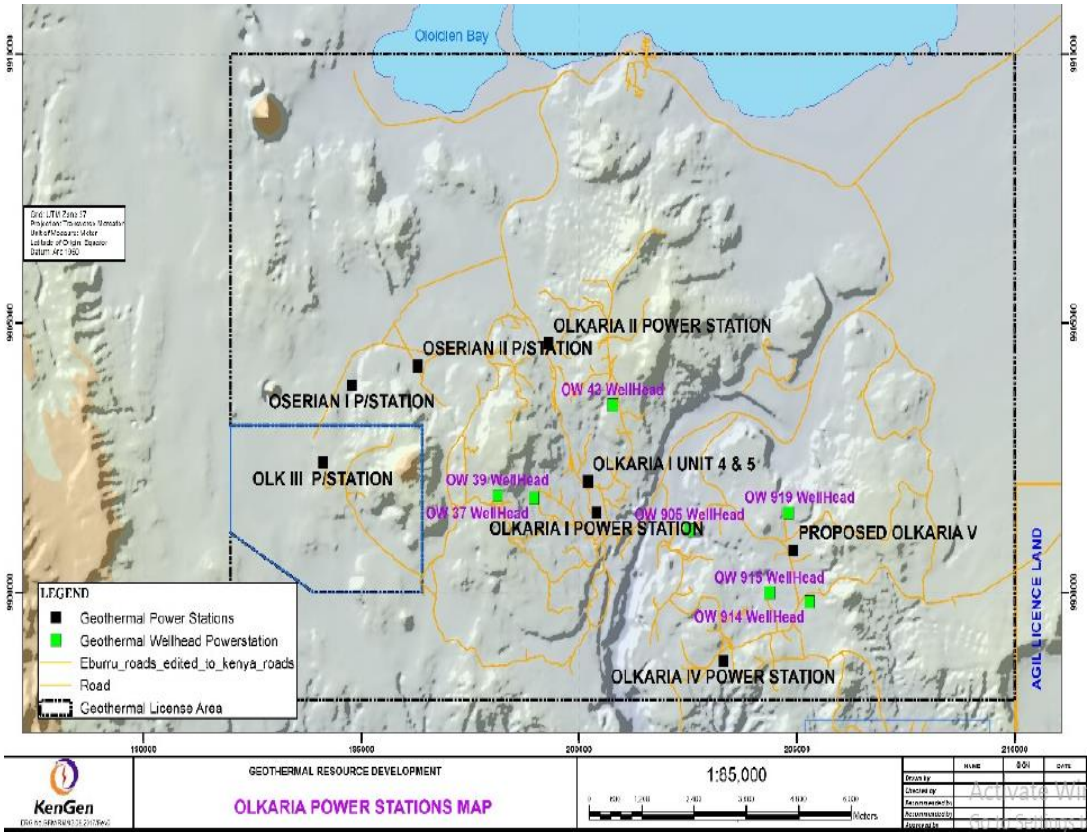

Figure 2.1: Map showing the locations of wellhead plants in the Olkaria geothermal fields (Source: Imaidi, 2017)

Structures present in the Greater Olkaria volcanic complex include; the Olkaria fault, Gorge Farm faults, Suswa lineament, and the Ol'Njorowa Gorge. The faults are prominent in the Olkaria Central and Olkaria West fields but are scarce in the Olkaria Domes area, possibly due to the thick pyroclastic cover. The NW-SE and WNW-ESE faults are thought to be the oldest and are associated with the development of the main Rift Valley (Opondo, 2008).

The Olkaria geothermal system is characterized by a liquid dominated reservoir though a single phase exists to the north of the Olkaria fault zone. However, a two-phase reservoir overlain by a vapor-dominated (steam) cap existed above the liquid reservoir in the Olkaria East sector when the first deep wells were sunk in the area (Karingithi et al., 2010). Olkaria reservoir fluids indicate the highest H_2O/CO_2 ratio except samples from Olkaria West that appear to spread along the H_2O-CO_2 axis. However, it is noted that high H_2O/CO_2 ratios appear to reflect relatively lower temperature fluids tapped from the shallower aquifers in the wells. This inference is made taking into account the different solute temperatures (particularly silica temperatures) of most of the wells discharging two-phase fluids (Malimo, 2013).

Olkaria fluid samples have also appeared to be slightly enriched in N_2 content. Differences in the N_2 content could be attributed to preferential nitrogen loss upon boiling, particularly in wells with high heat flow/content. It is also possible that air contamination could have occurred during sampling and/or due to the presence of drilling fluids in the reservoir and could be responsible for the N_2-rich samples, particularly for the wells which have been undergoing discharge testing until the present time. There are however other sources of N_2 in geothermal fluids. It has been observed from examination of well discharges that wells have N_2 and Ar concentrations of up to

ten times greater than that of air saturated water (ASW) and concentrations as low as one tenth that of ASW (Norman et al., 2001). Furthermore, studies in Iceland have shown from N_2/Ar ratios that N_2 has another source than air-saturated water, potentially entrapped air bubbles, magmatic gas or decaying organic matter (Giroud, 2008).

Olkaria wells on the other hand appear to be depleted in H_2 relative to Menengai. Menengai well MW-13 is the richest in H_2, having CO_2/H_2 ratios lower than 6, while fluids of wells MW-03 and MW-01 are the poorest in H_2, with CO_2/H_2 ratios higher than 30 and 70, respectively. Most fluids of Olkaria wells and fluids of wells MW-04, MW-06, MW-09, MW-19, MW-12 and MW-20 have intermediate characteristics, with $6 < CO_2/H_2 < 30$. High H_2 is usually taken to indicate the presence of vapor fraction in the initial reservoir fluid, which raises much the sparingly water soluble H_2 concentrations in the aquifer liquid but not so much the concentrations of the more soluble CO_2 and H_2S (Arnórsson et al., 2010). It is hence concluded that a high vapor fraction exists in the Menengai relative to the Olkaria reservoir.

CH_4 contents are distributed with most samples falling between CO_2/CH_4 ratios of 40 to 1200 units. Variations from field to field as well as from well to well in the contents of H_2 and CH_4 might be related to the existence of different redox conditions, temperature, pressure, and vapor/(vapor + liquid) mass ratio (referred to as y value) in the zones where gas equilibration is attained. Since H_2 and CH_4 are minor components, they are expected to be affected by chemical reactions, particularly hydrogen, which is highly reactive, rather than methane, which is considered a “slow” species, especially at relatively low temperatures.

It has been demonstrated that the concentrations of reactive gases H_2S and H_2 in the Olkaria reservoir fluids are generally kept in local equilibrium with pyrite-pyrhotite-

magnetite mineral assemblage. Furthermore, the CO_2 is controlled by close approach to local equilibrium with Epidote-prehnite-calcite-quartz mineral assemblage in most parts of the geothermal field except in Domes and Olkaria West where its concentration is controlled by its flux from the magma heat source. Furthermore, it was observed that the mineral assemblage pyrite–pyrrhotite–magnetite controls aquifer water H_2S and H_2 concentrations (Karingithi et al., 2010)

2.3 Effect of Various Geothermal Fluids Components on Turbines

Geothermal steam contains various solid particles resulting in particle erosion and scale deposits in turbines. It also contains hydrogen sulphide (H_2S) and carbon dioxide (CO_2), both of which are highly corrosive promoting aggressive corrosion in turbines. There are various variables affecting the corrosion rate of the geothermal fluid. These are; pH, dissolved oxygen, carbon dioxide, hydrogen sulphide, ammonia, sulphate, chloride and suspended solid material and its deposit (Ashree Technical Committee, 2002).

2.4 Erosion/Corrosion on Geothermal Power Plants

Several different mechanisms of metal destruction in the working path of geothermal power plants are possible depending on the hydrodynamic conditions, thermodynamic and phase state and also on the chemistry of the geothermal fluid. The fluid moves through the geothermal cycle and changes its thermodynamic parameters; phase state and physical/chemical state affecting the composition, conductivity and other parameters in the flow varying the potential for corrosion/erosion. These characteristics have to be considered when analysing erosion and corrosion processes. Erosion/corrosion is an interdependent process, involving formation of a protection layer of corrosion products on the metal surface, and hydrodynamic (mechanical) destruction and dissolution under the influence of flow. In other words

erosion/corrosion is a physical-chemical process, where corrosion and erosion factors are similar in magnitude and occur simultaneously. When studying the erosion-corrosion process in a geothermal fluid, it is necessary to consider redistribution of admixtures and gases between steam (main flow) and liquid (liquid film) phases (Povarov and Tomarov, 1997).

More than 70% of world's installed Geothermal Power Plants operate on a two- phase (wet-steam) heat carrier. Owing to interphase redistribution of substances, the major part of admixtures and salts is in the liquid phase and non-condensable are contained in the vapour phase. The phase state of the geothermal working fluid and the concentration of admixtures and non-condensable gases, taken in combination with the flow hydrodynamics and the erosion/corrosion properties of metal are the factors that determine to a considerable degree the possible occurrence and intensity of damage inflicted to Geothermal Power system components, as well as the formation of deposits on the surfaces of equipment and pipelines (Tomarov et al., 2012).

The physical/chemical properties and the concentration of admixtures and non-condensable substances determine the location of zones and intensity of erosion/corrosion, thinning and formation of deposits in the working loop. They also have an effect on the metal corrosion and cracking processes in the Geothermal Power Plant equipment. The mechanisms of droplet impingement and cavitation erosion depend on them to a lesser extent (Semenov et al., 2002).

Erosion/corrosion thinning and stress corrosion cracking of metal are the main factors causing abrupt fractures and failures of equipment and associated pipelines in Geothermal Power Plants and formation of deposits degrades their performance efficiency (Tomarov et al., 2012). Magnesium silicates are formed upon heating silica

containing ground water or mixing of cold ground water and geothermal water. They have been shown to consist mainly of poorly developed antigorite. Their solubility decreases with increased temperature and pH, hence increased deposition. However, the rate of deposition has been found to increase linearly with supersaturation but exponentially with temperature (Gunnarsson et al., 2005).

Depending on the chemical properties of the geothermal fluid, some ions precipitate and accumulate on the metal surface of the equipment. These accumulations have pores and tendency for forming cracks. In the case of release of those accumulations from the metal surface and with the presence of Cl ion, local corrosion occurs. Protective plating can be used on surfaces to prevent corrosion. Sulphur - stress breaking can be seen in steel materials which are subjected to hydrogen sulphide under stressed condition with water rich environment. Therefore, it shows that various conditions affect erosion/corrosion as follows;

2.4.1 Effect of pH

Corrosion/Erosion rate increases as pH decreases. This phenomenon is specifically experienced under acidic environments where the pH falls 7. The passivity of many alloys depends on pH corrosion increases with passivity breakdown. These conditions also facilitate pit corrosion which may result in stress corrosion cracking (Sanada, 2000).

2.4.2 Effect of Chlorides ions

Presence of chloride ions causes the breakage of the passive layer that is a protective layer preventing metals from corrosion. By breaking this layer, pit corrosion and cracking with stressed corrosion occurs (Thomas, 2003).

2.4.3 Effect of hydrogen sulphides

Hydrogen sulphide basically affects copper and copper-nickel alloys. Although usage of copper and copper-nickel alloys is advantageous in sea water environments, they are not preferred in geothermal fields because of the corrosion effect. In iron-based materials they are harmful above concentrations of 50 ppm. High strength steels are generally exposed to stress corrosion cracking by the effect of hydrogen sulphide. The H_2S also creates hydrogen bubbling in steels. If geothermal process fluid contains dissolved oxygen, hydrogen sulphide is oxidized with this oxygen and by decreasing pH of the geothermal fluid; it increases the corrosive features of the environment (Thomas, 2003).

2.4.4 Effect of sulphate ions

There is insignificant effect of sulphate ions on geothermal fluids. In the fluids containing low amount of chloride ions, sulphate acts as the main attacker ion but it is less effective hence minimal damage through erosion/corrosion (Thomas, 2003).

2.4.5 Effect of suspended solids

The existence of suspended solid materials in the geothermal fluid formed through precipitation of ions by chemical reactions causes deposit formation on the materials. Some of these solid materials result from loose rock particles within the earths' crust and are abrasive. The following types of metal destruction may take place in geothermal power plants through physical means;

(Povarov, et al., 1992)

i. General corrosion (GC)
ii. Pitting corrosion (PC)
iii. Contact corrosion (CC)

iv. Erosion-corrosion wears (ECW)

v. Corrosion cracking under load (CCL)

vi. Drop impact erosion (DIE)

vii. Cavitation erosion (KE)

viii. Abrasive erosion (AE).

Studies have shown that up to 40% of failures and emergency shutdowns of Geothermal Power Plants are connected to the failures of turbine components and working blades. The main cause of these failures is metal corrosion cracking (MCC) under cyclic tensions. Cracking is promoted by chloride in non-uniformity of salt deposition and pitting (Povarov *et al.*, 1991).

2.5 Scaling/Deposition on Geothermal Power Plants

The formation of amorphous silica scales in geothermal applications occurs in two mechanisms;

- Direct deposition or monomeric deposition,
- Colloidal deposition,

Direct deposition depends on the interaction of siloxane bonds of the silicic acid to the metal surface. This reaction occurs at high pH levels (pH > 8) and is catalyzed by hydroxyl ions. It produces a hard, dense and vitreous layer estimated to be contributing 0.5mm/yr. of scale (Sinclair, 2012). On the other hand, colloidal deposition occurs via a condensation-polymerization mechanism from silicic acid due to increasing saturation/supersaturation. This formation pathway forms small molecular weight dimers and trimers prior to forming rings of various sizes, and cross-linked polymeric chains and ultimately a complex and amorphous product (Amjad, 2010). After the polymerization stages, coagulation and flocculation further promotes the formation of much larger colloid particles (Bergna & Roberts, 2006).

Deposition is mainly affected by the silica concentration, temperature and pH; flow rates, aeration and ion effects are also important factors. The operating conditions are maintained at the no scaling zone (Brown, 2011). Numerous mitigation measures have been tested and are summarized as follows (Sinclair, 2012):

a. Addition of silica scale inhibitors and dispersant dilution of the brine with freshwater,
b. pH reduction to reduce the kinetics of polymerization,
c. Addition of dispersing/inhibiting agents to prevent silica side-reactions,
d. Removal of silica via induced precipitation, and cooling or rapid thermal quenching

Silica deposition occurs at different depths in various forms, these include quartz, chalcedony, crystallite, and amorphous silica. Quartz is the most stable form of silica, and has the lowest solubility. Deep geothermal water is usually in equilibrium with quartz at the prevailing reservoir temperature. Deposition of quartz in wellbores and surface equipment is not a common problem due to the slow rate of formation. Amorphous silica is, however, associated with changes in temperature of the geothermal water. This is when steaming extraction and fluid cooling takes place. Deposition of amorphous silica from supersaturated water is, thus, the most troublesome scale when precipitated on the surface equipment such as pipelines, separators, turbine nozzles, heat exchangers and re-injection wells. This problem is more troublesome in high-enthalpy geothermal fields as steam separation is taking place there and because of higher initial silica concentrations. In most fields, the steam separator is operated below the amorphous silica line (under- saturated) so as to avoid silica scaling in the pipelines and separator. Operation above the amorphous silica line

will cause scaling but at very different rates, depending on the water composition, retention time and other factors (Axelsson & Gunnlaugsson, 2000).

The deposition of calcium carbonate from a geothermal fluid is a major problem in a number of geothermal fields, mainly due to plugging of geothermal wells. The most common polymorphs of calcium carbonate minerals are calcite, aragonite and vaterite. Vaterite is the first mineral to form in a supersaturated calcium carbonate solution, but is apparently unstable, recrystallizing to form the more stable calcite. Hence, the most frequently occurring calcium carbonate deposition minerals are calcite and aragonite with the former dominating (Arnorsson & Stefansson 2007).

The mechanism responsible for the formation of sulphide deposition is different in low- and high-enthalpy geothermal fluids. Low-enthalpy fields containing high concentrations of dissolved solids could cause mild corrosion of steel production casings, which liberates iron. Therefore, the migrated iron, due to corrosion, reacts rapidly with sulphide- rich geothermal fluids that produce a higher deposition rate of metal sulphide scale. In a high-enthalpy geothermal system, sulphide mineral deposition is due to sulphide-forming metals such as iron and some other base metals (Fe, Zn and Pb). When sulphide forms on nickel and chromium as secondary products, there is a probability of troublesome scale occurring, causing localized corrosion or sulphide stress corrosion cracking. Sulphide depositions in high enthalpy resources can be severe in water with high Total Dissolved Solid (TDS) content since it combines with silica scaling. In high-enthalpy systems, metal sulphides and oxides are frequently deposited directly from the geothermal fluids upon a change of phase or pH (Criaud & Foulliac 1989).

Sulphur forms a solid deposition in surface equipment in a similar way as formed around fumaroles. Sulphur deposits from geothermal fluids rich in H_2S gases, and causes operational troubles in power units, especially in condensers and cooling towers. Sulphur exchanges between sulphate and hydrogen Sulphide depending on its concentration, pH and temperature. The reaction is rapid under acidic conditions, but is very slow in alkaline environments. Elemental Sulphur (S) is deposited in direct contact condensers, where gases come into contact with oxygen; Sulphur can also plug the water distribution nozzles on top of cooling towers (Kristmannsdóttir et al., 2000).

The geothermal fluid is let into the power units through geothermal wells and pipelines. Depending on the temperature and pressure of the fluid, it can initiate boiling in the reservoirs or liners and wellbore, causing precipitation of solids. For instance, with calcite precipitation the formation mechanism is due to gases being liberated from the liquid phase and degassed into the steam phase. This causes super-saturation and calcite starts to precipitate inside the wellbore which, in time, results in fluid obstruction. This deposition causes a reduction of the flow area and, thus, a decline in well output, i.e. wellhead pressure drop (Ormat, 2001).

2.6 Chemical Characterization of Geothermal Fluids

Chemical characterization of geothermal fluid samples are the primary data source used by geochemists to gain an understanding of geothermal systems. The methods of analysis commonly used are a mixture of modern instrumental techniques such as atomic absorption spectroscopy and classical titrimetric procedure. Two instrumental multi-element methods described in the literature of the mid-seventies appear to be ideally suited for the analysis of geothermal waters and condensates. Inductively

coupled plasma spectroscopy and ion chromatography (IC), are both capable of rapid multi-element analyses on small sample volumes over a wide concentration range.

2.6.1 Inductively coupled plasma spectroscopy

Inductively coupled plasma spectroscopy (ICP) is basically an emission technique combined with a unique source, an argon-supported, inductively coupled. Atomic emission spectroscopy has been used for quantitative analysis since the 1930's and the development of inductively coupled plasmas began in the forties. It was not until the plasma's potential as a spectroscopic source was fully appreciated and developed. Operating at atmospheric pressure and at temperatures that range from 6,000 to the plasma serves as a nearly ideal vaporization atomization-excitation-ionization source for the optical spectrometer.

ICP spectrometers are available in two formats, simultaneous or sequential, depending on whether the spectrometer portion uses a polychrometer or a monochrometer, respectively, to separate the emission lines. Argon from compressed gas cylinders is splitting to three, flow- controlled supplies. One of these operates the pneumatic nebulizer which introduces the sample in to the plasma and to provide a cooling sheath between the plasma and the walls of the quartz torch. Light energy from the sample atoms excited by the plasma is focused onto the primary or entrance slit of the polychrometer. In addition to the primary slit, the polychrometer consists of a concave diffraction grating and a series of secondary or exit slits, all of which are mounted on an arc port of a 1-meter focal length circle. Each exit slit is precisely located to select a particular spectral line for one of the elements of interest. Light passing through these slits is focused by mirrors onto photomultiplier tubes where it is converted into electrical signals proportional to the emission intensities and thus the amount of the

individual elements present in the sample. Through the measuring instruments and the computer, these signals are printed out as concentration units at the operator's terminal.

The greatest advantage of ICP spectroscopy relative to other methods of analysis, whether multi-element or not, is its ability to determine, rapidly, a large proportion of the elements that appear in the periodic chart at concentrations spanning trace to major levels, without the need to adjust or change any instrumental operating parameters. In addition, the method is essentially free from chemical and ionization interferences; hence can be applied to sample of very low volumes and provides results with acceptable levels with precision and accuracy.

2.6.2 Chromatographic techniques

Chromatographic techniques have become the most powerful means available for laboratory analysis for the separation of mixtures of similar chemical species. In many cases an appropriate detector is combined with the chromatographic separator to produce an instrument capable of qualitative and quantitative determinations. Chromatography operates by distributing the sample components between a stationary phase, the ion exchange resin, and a mobile phase, the suitable ionic solution or eluent. In the usual arrangement, the stationary phase is packed in a column and the sample is forced down the column by the eluent solution, resulting in a differential migration of the sample components.

Separation of sample anions is determined by the degree to which they are attracted to these active sites. Ions with a low affinity are eluted more rapidly and produce narrower peaks than those with a strong affinity for the active sites on the resin. The next column is the suppressor or stripper column, which contains a high capacity, strong acid and cation exchanger resin. As the highly conductive eluent ions pass through the

suppressor, they are converted to a low conductance, weak acid form. For example, the sodium bicarbonate eluent used is converted to carbonic acid. After leaving the suppressor column, the separated anions of the sample pass through the conductivity cell of the detector. The resulting detector signals are monitored on a conductivity meter and can be used to trace a chromatogram or feed an integrator to provide the identification and concentration of the sample species or both.

2.7 Analysis of Solid Scales/Deposits using X-ray diffraction (XRD)

The atoms are arranged in a regular pattern, and there is as smallest volume element that by repetition in three dimensions describes the crystal. This smallest volume element is called a unit cell. The dimensions of the unit cell are described by three axes. The X-ray diffraction pattern of a pure substance is, therefore, like a fingerprint of the substance. The powder diffraction method is used for characterization and identification of polycrystalline phases. Diffraction patterns have been collected and stored on magnetic or optical media as standards. The main use of powder diffraction is to identify components in a sample by a search/match procedure; the areas under the peak are related to the amount of each phase present in the sample (Meier, 2001).

When an X-ray beam hits an atom, the electrons around the atom start to oscillate with the same frequency as the incoming beam. In almost all directions there will be destructive interference, that is, the combining waves are out of phase and there is no resultant energy leaving the solid sample. However the atoms in a crystal are arranged in a regular pattern, and in a very few directions we will have constructive interference. The waves will be in phase and there will be well defined X-ray beams leaving the sample at various directions. Hence, a diffracted beam may be described as a beam

composed of a large number of scattered rays mutually reinforcing one another. The figure 2.2 can be used to illustrate the principle of operation of XRD.

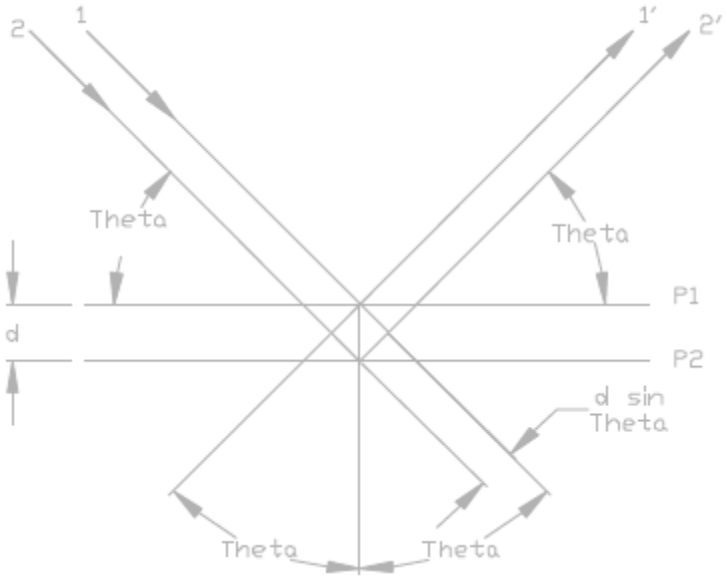

Figure 2. 2: Principle of operation of XRD
(Source: Meier, 2001)

An X-ray beam is directed incident to a pair of parallel planes P1 and P2, separated by an inter-planar spacing d. The two parallel incident rays 1 and 2 make an angle (THETA) with these planes. A reflected beam of maximum intensity will result if the waves represented by 1' and 2' are in phase. The difference in path length between 1 to 1' and 2 to 2' must then be an integral number of wavelengths (nx). This relationship can be expressed mathematically using Bragg's law stated as:

2d x sin T = n x …… *(Equation 2.1)*

A typical diffraction spectrum consists of a plot of reflected intensities versus the detector angle 2-Theta or Theta depending on the goniometer configuration. The 2-Theta values for the peak depend on the wavelength of the anode material of the X-ray tube. It is therefore customary to reduce a peak position to the inter-planar spacing d that corresponds to the h, k, l planes that caused the reflection. The value of the d-spacing depends only on the shape of the unit cell. The d-spacing is obtained as a

function of 2-Theta from Bragg's law. Upon the determination of the d-spacing, International Center for Diffraction Data (ICDD), which is the organization that maintains the data base of inorganic and organic spectra, will then be used for search/match techniques to identify the sample using computer software.

2.8 Impacts of the Subject Defects on Turbine Performance

At Olkaria's well head power plants, 23 incidences have been observed in a period of five years resulting in forced shut down of the plant units (Kengen's Reports, 2019). All these incidences are as a result of turbine failures related to corrosion/erosion and deposition/scaling defects observed during maintenance to restore the plants back to operation. The summary of this information is indicated in table 2.1.

Table 2. 1: Summary of failures observed at Olkaria's well head Power plants

Incident	No. of occurrence	Possible cause	Defect causing failure
• Fractured rotor blade	4	• Material defects. • Stress concentration on root of the blade. • Corrosion cracking failure	• Corrosion and erosion
• Severe corrosion on the diaphragms	10	• Material defects	• Corrosion and erosion
• Erosion on the rotor Surface	2	• Inferior material selection. • Moisture carry over due to poor separation of steam	• Corrosion and erosion
• High vibrations due to rotor imbalance resulting from deposition and uneven corrosion	1	• Scaling on rotor surface leading to uneven build-up of mass on rotor. • Corrosion leading to uneven loss of mass from rotor.	• Deposition/Scaling • Corrosion and erosion
• Rotor bending	4	• Inadequate burn-in tests during design. • Imbalances arising from uneven mass build up and losses in the rotor. • Reverse power operation. • Fatigue arising from sudden trips.	• Deposition/Scaling • Corrosion and erosion
• Steam gouged casing and diaphragm surfaces	2	• Material defects	• Corrosion and erosion

(Source: Kengen Reports, 2019)

Some of the corrective actions undertaken by Kengen to remedy the failures include:

- Straightening of rotors using off-set machining technique, spotting technique (thermal method) and dynamically balancing of the rotors. All these services are outsourced; hence time consuming as the rotor has to be transported to workshop for repair. The exercise is highly expensive as it involves both procurement and logistical procedures. As a result the plant availability and reliability is highly affected. Since the plant's overall efficiency is indirectly dependent on these factors, then it is greatly reduced.
- Re-blading of affected turbines. This basically involves the replacement of the affected blade with new spares. This is a temporary solution and is highly dependent on the availability of the spares. In case there is none available in store, then the plant will always remain under shut down. Plant availability as well as reliability will be affected.
- Cleaning by sandblasting – To be able to carry out this activity, the plant should be overhauled. The process is usually tedious and time consuming. On the other hand, repeated cycles of sand blasting on the turbine increases erosion through abrasion as it act as a source of flaws on the surface that can easily propagate in to a fracture. This will basically affect the equipment's life span.

Based on the data indicated in table 2.1, it is clearly shown that the subject defects have a huge impact as far as power generation is concerned. On the other hand, repeated cycles of incident occurrence indicate that permanent solutions have not been implemented. This therefore means that such failure may reoccur in future. However, this is an undesirable situation as repetitive recurrence of failures impacts highly on the life span of the equipment which necessitates a permanent and reliable solution. It is

for this reason therefore that this research study was carried out to find possible solutions through root cause analyses aiming at reducing or eliminating the subject defects and subsequent failures which will reduce break downs and forced shut downs; hence improving on the plant's performance, availability, reliability and most importantly extend the life span of the turbine sets through reduced cycles of failures.

2.9 Manufacturing Methods of Preventing Corrosion/Erosion in Turbines

Turbine manufacturers in their quest to enhance their turbine efficiencies and reliability have developed technologies to counter cases of erosion/corrosion. These technologies focus on the design and manufacturing stages and they include the following;

2.9.1 Coating Technology

Turbine parts such as blades, diaphragms and the rotor itself are exposed to highly corrosive geothermal steam during operation. These parts are susceptible to erosion/corrosion that may lead to the problem of dropout of the seal pin between blades causing catastrophic failure. To prevent this, thermal spray coating is used to protect the part's surface. Previous research done on corrosion testing in a modelled geothermal environment have shown that WC-CoCr material has excellent corrosion resistance as a flame spray material (as illustrated in table 2.2) suitable for practical application of geothermal steam turbines (Sakai et al., 2005).

Table 2. 2: Coating test results

Coating material	Stress corrosion cracking (SCC)	Fatigue	Corrosion weight reduction	Blast erosion (amount of average wear)	Hardness Hv
CoNiCrAlY+ $Al_2O_3 \cdot TiO_2$	Poor	Poor	Excellent	Good	790
WC-10Co4Cr	Excellent	Excellent	Excellent	Excellent	1,100
CoCrMo	Poor	Fair	Excellent	Good	650
Al-Zn	Poor	—	—	—	—
Stellite No. 6B spraying	—	—	Poor	Good	540
50 % Cr_3C_2-50 % NiCr	Excellent	Fair	Fair	Good	770
75 % Cr_3C_2-25 % NiCr	—	—	Fair	Good	810

— : Not tested

(Source: Sakai et al., 2005)

This technology utilizes the HVOF (High-Velocity Oxygen-Fuel thermal spray coating, High-Velocity frame spraying) process to apply a coating of WC-CoCr thermal spray material on the surface of the turbine parts; hence protecting them.

2.9.2 Shot Peening Technology

Interfaces between the blades and the rotor are the blade root and rotor groves which acts as crevices or gaps between which corrosive materials from geothermal steam may accumulate. This causes SCC and corrosion fatigue in the turbine parts. Based on the results of a previous research on turbine manufacturing material, the recommended materials for the blades and the rotor should be highly resistant to both SCC and corrosion fatigue (Sakai et al., 2005).

In order to endure more severe corrosive environment and higher stresses, shot peening technology is utilized due to its capability to withstand such conditions. The technology

bombards the high-stress areas of the blade and rotor with steel balls at high speed so that compressive residual stress is generated in the surface of the part, thereby enhancing the capability to withstand SCC and corrosion fatigue (Sakai et al., 2009).

Results from a previous study on SCC and corrosion fatigue tests done on shot-peened blade and rotor materials verified their longer life as illustrated in figure 2.3. Significant improvement in resistance to corrosion was confirmed as the time to failure was at least twice as long for shot-peened material as compared to the one that wasn't shot-peened. This therefore reaffirms shot peening technology as an effective measure to increase the life of steam turbines due to increased resistance to corrosion (Sakai et al., 2005).

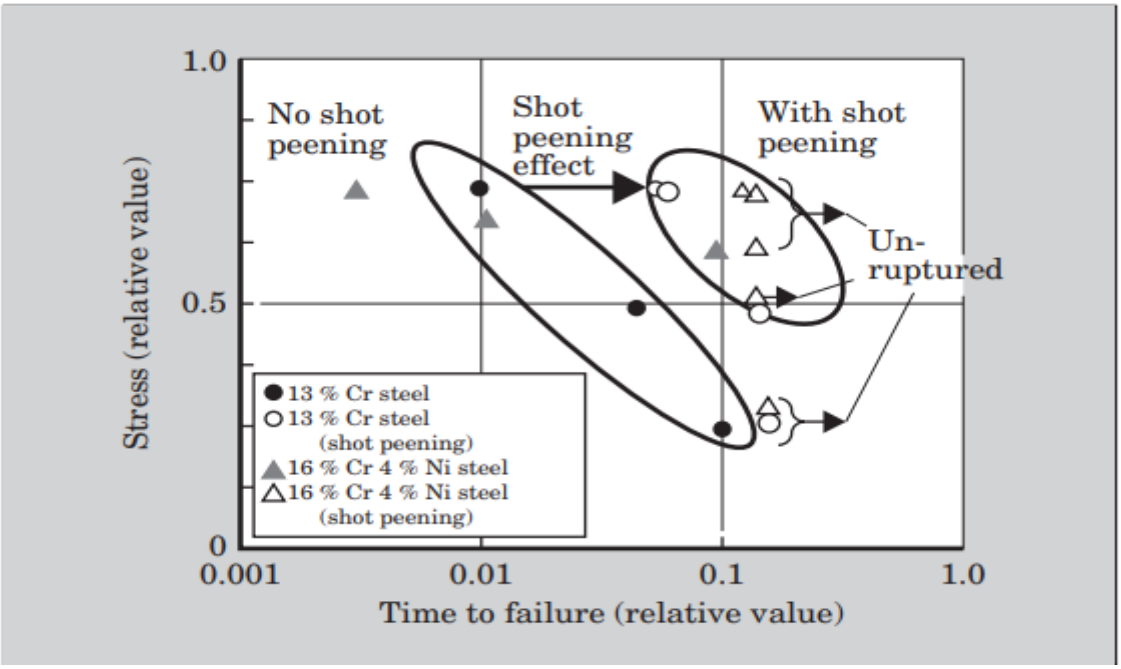

Figure 2. 3: SCC Test Results
(Source: Sakai et al., 2005)

2.9.3 Material Technology

Geothermal steam turbines usually operate under much more severe environmental conditions than those of ordinary steam turbines in other types of power plants. Its material resistance to corrosion is a crucial consideration for the stable long term

operation of the turbine under such conditions. Through corrosion testing in a modelled geothermal environment and simulated geothermal fluid conditions, suitable materials were selected for practical applications.

Based on the verification results from various material tests, standard materials for geothermal turbine-use and optimal materials were selected according to the working environment, stress and other usage conditions as shown in table 4.9 (Sakai et al., 2009).

Table 2. 3: Standard Materials for geothermal turbines

Part	Standard material
Blade material	13% Cr steel 16% Cr-4% Ni steel Ti-6% Al-4% V alloy
Rotor material	1% Cr-MoNiV steel 2% Cr-MoNiWV steel

(Source: Sakai et al., 2009)

CHAPTER THREE

RESEARCH METHODOLOGY

3.1 Geothermal Fluid Sampling and Treatments

Sampling of geothermal fluids were done from three selected points; before separation, after separation and at the exhaust after the turbine as shown in figure 3.2. The samples were collected from two selected power plants, for three days each, giving six days' set of results as tabulated in Appendix I. An average of the six days' results at each collection point were calculated and presented in table 4.1 as a representation of all the well head power plants. Collection of steam and water samples were done using a chromium steel Webre separator attached to selected points along the steam line of the wellhead plants using a horizontal discharge testing technique. The design of this apparatus is as illustrated in the figure 3.1.

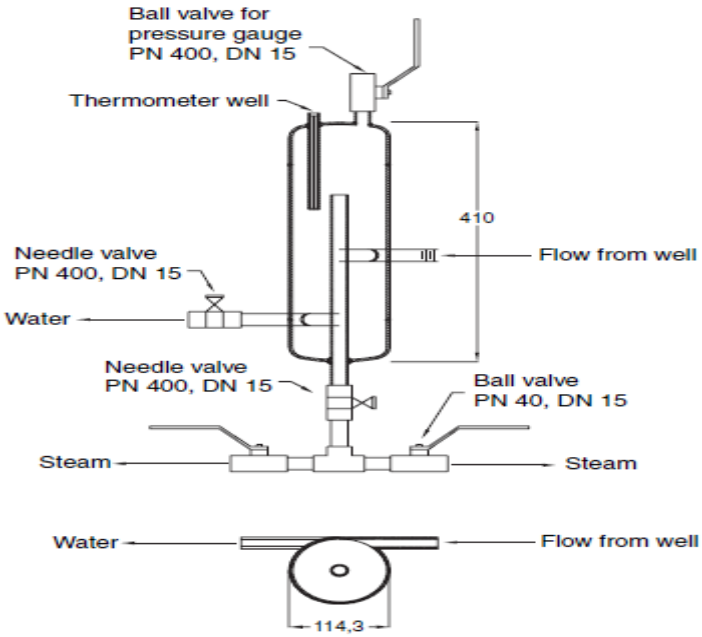

Figure 3. 1: Design of a Webre separator
(Source: Arnorsson et al., 2006)

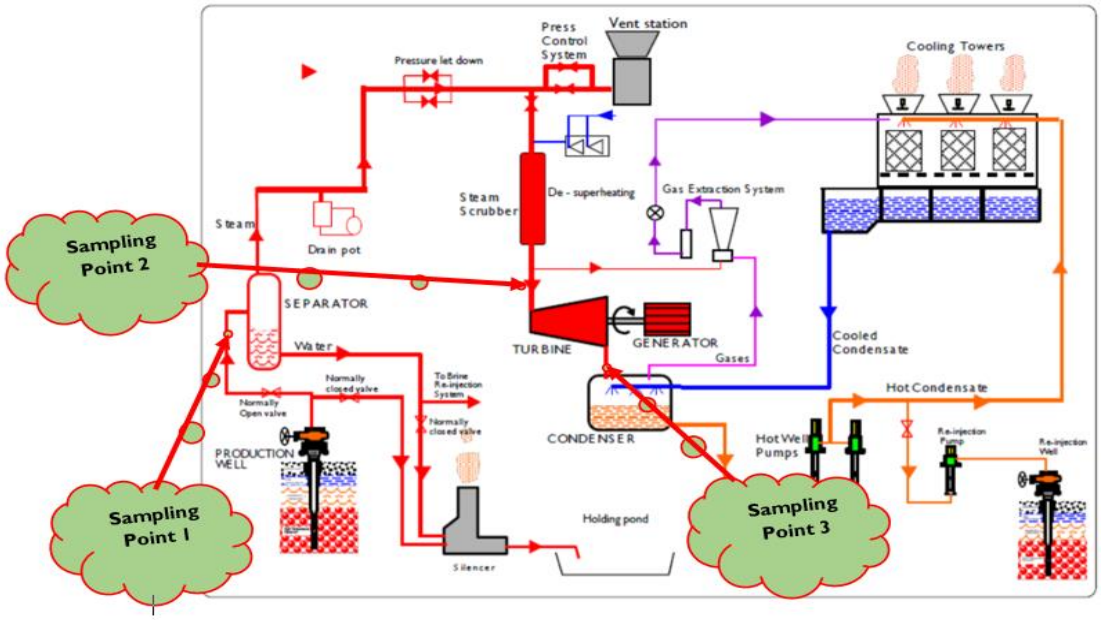

Figure 3. 2: Sampling points location in the power plant
Source: Researcher 2019

Before sampling, some of the steam was pumped through the sampling apparatus for purposes of cleaning and to remove any contaminants. The equipment for the sampling of geothermal fluid from a geothermal system using a Webre steam separator were set as illustrated in the following figures.

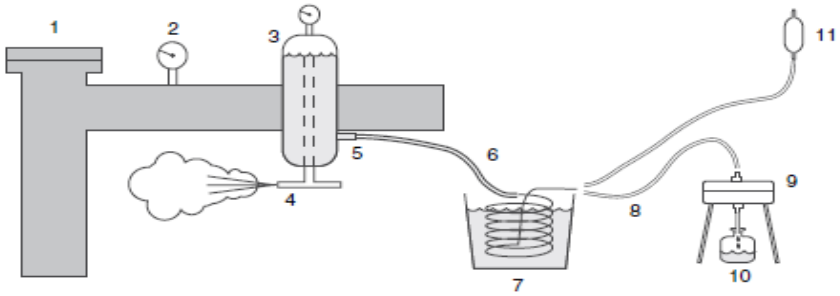

Figure 3. 3: Sampling of the liquid phase of the geothermal fluid and dissolved gases
(Source: Arnorsson et al., 2006)

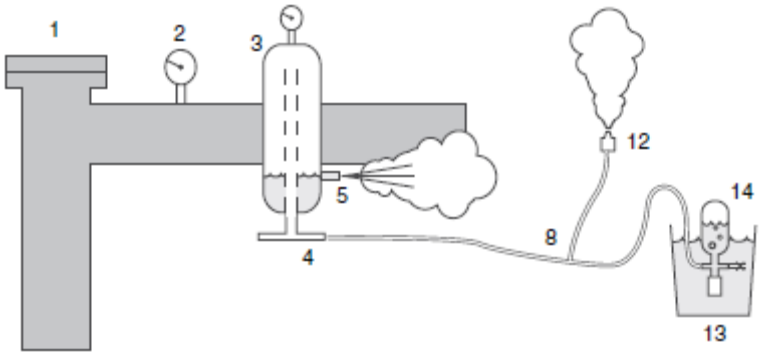

Figure 3. 4: Sampling of the dissolved gases in the steam/ gaseous phase of the fluid
(Source: Arnorsson et al., 2006)

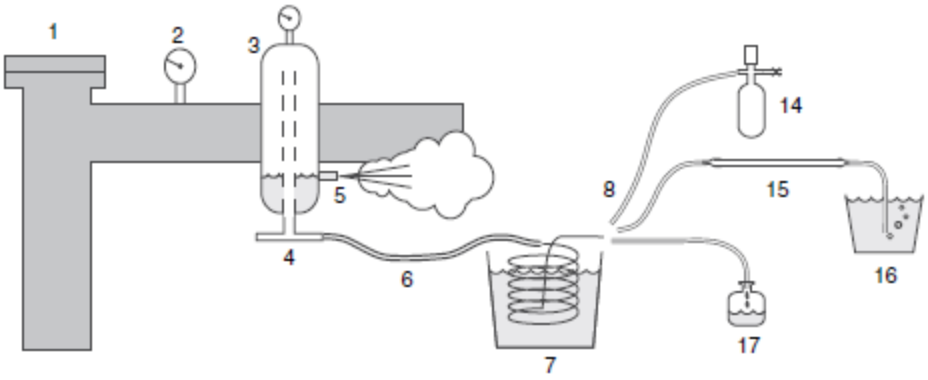

Figure 3. 5: Sampling of the fluid in vapor form
(Source: Arnorsson et al., 2006)

Where;

1. Wellhead.
2. Pressure gauge.
3. Webre steam separator.
4. Steam outlet valve.
5. Water outlet valve.
6. Steel-clad Teflon tubing.
7. Bucket with cold water and cooling coil (approximately 6 m long) of stainless steel (N316).

8. ¼ inch diameter thick-walled silicone tubing which may be either connected to the filter holder or to a gas sampling bulb with stopcocks at both ends.
9. Teflon filter holder with 20 cm diameter 0.2 l m filter membrane.
10. Sample bottle.
11. Gas sampling bulb with stopcocks at both ends, 300 ml, for determination of pH
12. One-way atmospheric valve.
13. Bucket with cold water.
14. Gas sampling bulb, 300 ml.
15. Copper tubing (approximately 30 cm long), with special clamps at both ends, for the sampling of noble gases and individual gas components for isotopic measurements.
16. Small bucket with water to prevent air from entering the copper tubing.
17. Sample bottle for condensate for the determination of dissolved nitrites, hydrides and oxides

Samples for analysis of all components except for pH were filtered on site to prevent interaction with any suspended matter through 0.45 μm filter papers into low density polyethylene bottles using a polypropylene filter holder.

The liquid samples collected into polyethylene bottles were treated upon collection, depending on the analysis required. Samples used for the determination of pH, Total Dissolved Solids (TDS), conductivity, and Chlorine, were collected and stored without any further treatment. Samples for Silicon IV Oxide (SiO_2) analysis were diluted ten times using deionized water to avoid polymerization of monomeric silica.

Samples analyzed for cations and SO_4 were filtered through a 0.45 μm Millipore membrane. Cation samples were preserved with 1 ml nitric acid, while 1 ml of 0.2 M Zn-acetate solution was added to the samples for SO_4 analysis to precipitate the sulphides in the form of ZnS.

3.2 Geothermal Fluid Sample Analysis

Analysis of the liquid samples for determination of pH, Total Dissolved Solids (TDS) and conductivity were carried out promptly as soon as it was brought from the field. The Conductivity and pH were determined in the laboratory by potentiometric analyzer and a pH meter respectively. TDS was measured using a TDS meter.

Analysis of the aqueous cations (Na, and Fe) was done using the Atomic Absorption Spectrometer (AAS). The analyses of chloride, SiO_2 and SO_4 were done through spectrophotometric technique using Ultra-Violet/Visual light analysis.

3.3 Sampling and Analysis of Solid Samples

3.3.1 Sampling of the solid samples

Samples of scales/deposits were collected from surfaces of the turbine rotors, blades and diaphragms of identified plants during scheduled major maintenance operations. The sampling method used was mechanical scrubbing of the solid deposits from the selected points. Since all the locations are within the same steam chamber, the collected samples from each identified plant were mixed to form one sample. All samples were oven-dried at 105°C and cooled down using a desiccant humidifier before analysis.

A sample of 1st stage turbine blade was collected from a failed rotor and elemental analysis was carried out to determine the composition of the parent material.

3.3.2 Analysis and Characterizations of the Solid Samples

Instrumental analytical techniques were used to identify and characterize the solid samples. Qualitative and quantitative chemical analyses were carried out using the following methods:

a. X-Ray Diffraction (XRD analysis) – was employed to quantitatively analyze the compounds present in the scales/deposited materials.

b. X-Ray Florescence (XRF analysis) – was used to analyze the elemental composition of deposited materials and metal chippings from the turbine blade sample;
c. Metal Scan (using Metal Scanning Spectrometer) - was used to analyze a turbine blade sample to determine the elemental composition of the parent material ;

3.4 Determining the Cause of the Defects in Turbines

Following a comprehensive determination of geothermal fluid composition and characterization of the solid deposits in comparison with the turbine blade material of Olkaria's well-head plants, an inferential approach was adopted to study what causes the defects on the turbines. This approach focused on the quantities, operational behavior and characteristics of each element and compound found in the sampled fluid and deposits. The data collected and the knowledge from literature was then used to inform the causes of the defects and how they affect the plant's energy conversion efficiency and the resultant output.

3.5 Determining the Methods of Eliminating the Defects on Turbines

A review on the turbine design considerations and manufacturing standards guided the determination of effective solutions for preventing and eliminating the defects during the design and manufacturing stages.

3.6 Implementation of Selected Methods of Eliminating the Defects on Turbines

In this research, repair and maintenance approach was adopted by implementing hard facing and machining techniques. These techniques were determined as suitable methods of eliminating the defects and were used to refurbish a highly affected turbine. The procedures and considerations followed during the refurbishment, emulated the

recommendations of both design and manufacturing standards guided by literature as described in section 2.9.

The repair process involved extraction of 1st stage nozzles and seven pairs of diaphragms from top and bottom casings by gas heating, hammering and hydraulic jacking as shown in figure 3.6. This process was onerous but climaxed in successful extraction of all diaphragms. The extracted diaphragms and casings were cleaned of visible coatings as well as contaminants of carbon, rust and silica deposits to bare metal substrate. Diaphragms were inspected of cracks, deformations and scope of repair works determined. Chemical composition of alloying elements in carbon steel rings and stainless steel fixed blades, as indicated in tables 3.1 and 3.2, were established to pilot the selection of suitable filler metal to join stainless steel blades and carbon steel rings.

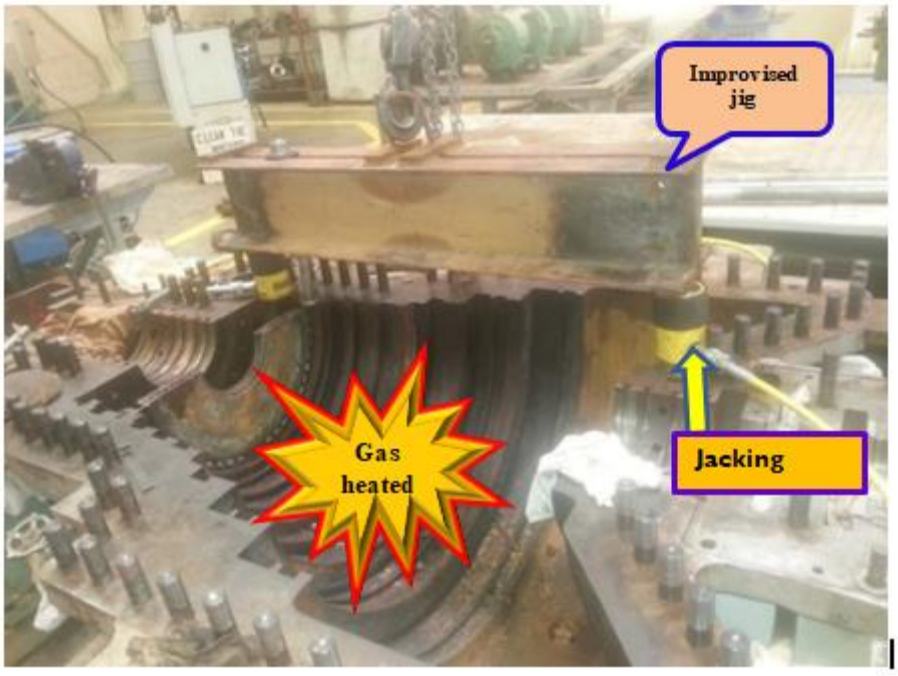

Figure 3. 6: Extraction of diaphragms
(Source: Researcher, 2019)

Table 3. 1: Chemical composition of hot rolled steel plates

IS 2062 Grade	C %	Mn %	S %	P %	Si %	C .E %
	Max	Max	Max	Max	Max	Max
B	0.22	1.5	0.045	0.045	0.40	0.41

(Source: Prosaic Steel & Alloys)

Table 3. 2: Mech. Properties hot rolled carbon steel plates

Grade	Yield Strength (MPa)	Tensile Strength (MPa)	Elongation %	Bent
B	240	410	23	3T (>25mm)

(Source: Prosaic Steel & Alloys)

A filler material suitable for joining carbon steel rings and stainless steel blades was selected and the desired welding method and conditions determined. A material composed of 23.9%Cr, 13.0% Ni, 1.8%Mn and 0.15%Mo (AWS A5.9:ER309L) was selected as a suitable overlay material for the repair in view of its fusion characteristics, toughness, tensile and creep strengths. The properties of the overlay material were as follows;

Table 3. 3: Chemical composition of the filler material

Elements	C %	Cr %	Ni %	Mo %	Mn %	Si %
Wire Composition	0.02	23.9	13.0	0.15	1.8	0.50

(Source: Lincolin Electric Company)

Table 3. 4: Recommended welding parameters

Dia. (mm)	Wire Feed speed (m/min)	Voltage (volts)	Current (Amps)
3.2	0.9~2.8	28~34	200~700

(Source: Lincolin Electric Company)

Table 3. 5: Mechanical Properties of filler metal

Yield Strength (MPa)	Tensile Strength (MPa)	Elongation %	Ferrite Number
400	575	35	8

(Source: Lincolin Electric Company)

To ensure proper fusion of the overlay material on to the parent material, TIG welding technique was selected as the most suitable welding method for the repair due to low heat input and high efficiencies associated with the process. Precautions were taken to avoid post weld defects. Stitch welds were applied diagonally at alternating intervals to avert occurrence of permanent distortions, warpage and cracks. Welded parts were cooled gradually in dry sand to reduce post weld residual stresses due to welding and hardening at heat affected zones (HAZ), which could cause stress corrosion cracks (SCC) under wet conditions. Welds were examined of cracks by NDT, root penetration and trimmed to running clearances. Dimensional checks were done to confirm that structural integrity of the diaphragms was not affected. Eroded and steam gouged surfaces were re-filled by welding and milled to recommended clearances for smooth directional flow of the steam during operation; hence improving on the turbines efficiency by reducing frictional losses. The refurbishment process was illustrated in the figures 3.6 to 3.13.

Figure 3. 7: Weld repaired diaphragm
(Source: Researcher, 2019)

Figure 3. 8: Milling of repaired diaphragm split line face
(Source: Researcher, 2019)

Figure 3. 9: Repaired Diaphragm
(Source: Researcher, 2019)

Figure 3. 10: Repaired diaphragm fitted with key lock and assembling bolt & nut
(Source: Researcher, 2019)

Figure 3. 11: Repaired and installed diaphragm with rotor
(Source: Researcher, 2019)

Figure 3. 12: Reassembled rotor after repairs
(Source: Researcher, 2019)

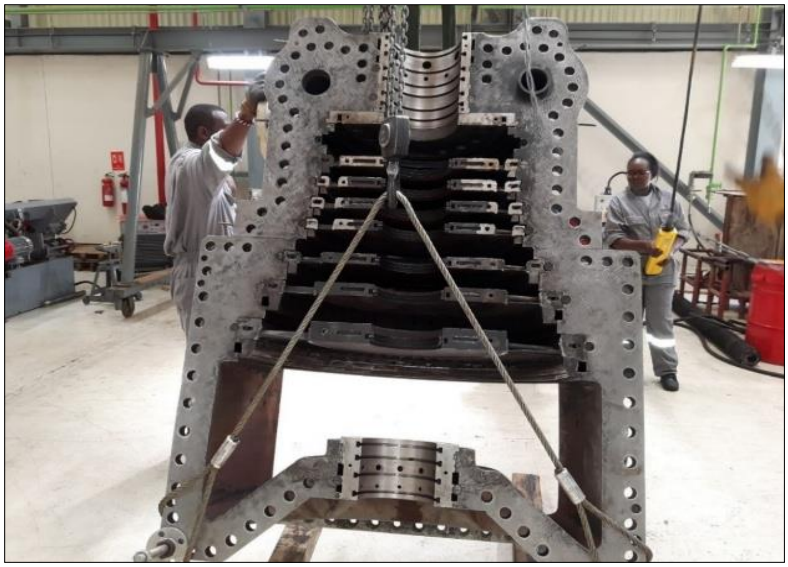

Figure 3. 13: Assembled Upper Casing after repairs
(Source: Researcher, 2019)

CHAPTER FOUR

RESULTS AND DISCUSSIONS

4.0 Introduction

This chapter basically focuses on the presentation of results and their discussions. The results indicate the composition of geothermal fluids sampled from three different locations (before separator, after separator and after the turbine), of well head power plants at Olkaria as well as characterization of solid deposits collected from the turbine blades, rotor and diaphragms. It also shows the elemental analysis of the turbine blade indicating the chemical composition of the parent material.

The discussions seek to illustrate how geothermal fluid composition and solid deposits' characteristics aid in the defects formation and subsequently, failures observed in the turbine sets of the well head power plants. It also seeks to illustrate whether the selected material for the turbine blade meets the recommended quality suitable for the application.

4.1 Determination of Geothermal Fluid Composition

Determination of geothermal fluid composition essentially involves three main steps. This includes:

- Collection and treatment of samples – as illustrated in Chapter 3 (section 3.1)
- Analyses of the samples – as illustrated in Chapter 3 (section 3.2)
- Interpretation of the data.

In this study, geothermal fluid samples were collected and analyzed for six different days and their results were tabulated as shown in Appendix I. The results were further processed and a summary given in the Table 4.1;

Table 4. 1: Summary of geothermal fluid composition for Olkaria's WHPs

LIQUID SAMPLE ANALYSIS									
MEAN VALUES									
	SAMPLING POINT	**pH**	**TDS(ppt)**	**CONDUCTIVITY (Us/cm)**	**CHLORIDE IONS (ppm)**	**SULPHATE IONS (ppm)**	**SiO2 (ppm)**	**IRON (mg/L)**	**SODIUM ion (mg/L)**
	1	5.36	304.17	608.33	233.27	37.30	75.40	1.31	187.00
	2	4.55	12.40	24.78	6.59	6.27	0.71	1.56	1.03
	3	4.79	5.30	10.67	3.52	3.23	2.96	0.89	0.17
KEY FOR SAMPLING POINTS:									
1	DIRECT FROM THE WELL/BEFORE SEPARATION								
2	AFTER SEPARATION/BEFORE TURBINE								
3	AFTER THE TURBINE								

(Source: Researcher, 2019)

The analysis in table 4.1 shows that each parameter of the sample composition, exhibits a given trend from one sampling point to another. However a common observation is that the values at sampling point 1 are significantly high as compared to those from sampling points 2 and 3. This is basically because the geothermal fluid directly from the well is usually in two phases mostly accompanied by other several matter like debris and gases. In order to admit it in to the turbine, the steam is passed through a separator which removes the liquid phase known as brine and all the solid material. The resultant steam should be pure and dry as much as possible but its quality depends on the efficiency of the separator. The trends as exhibited by each parameter are illustrated in the figures 4.1 to 4.8;

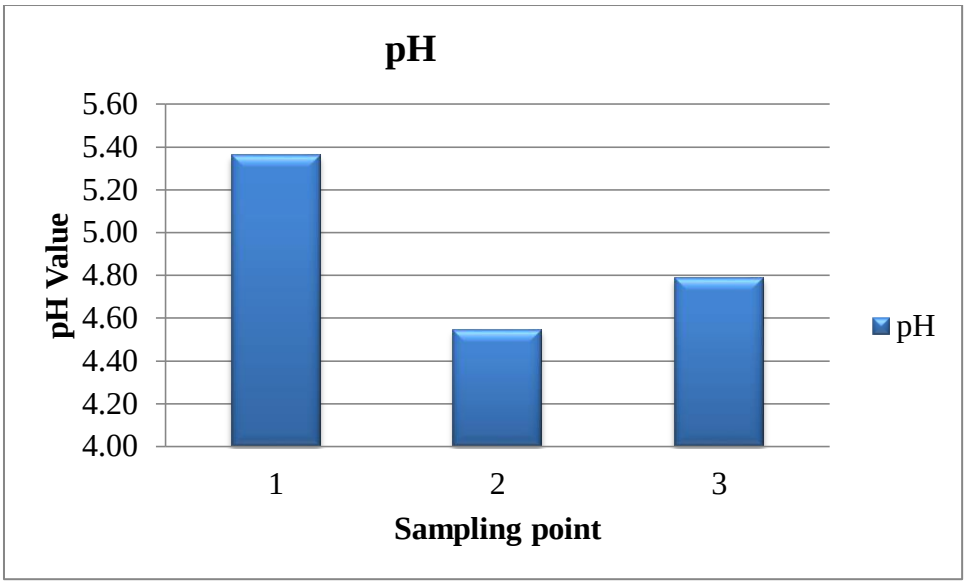

Figure 4. 1: Geothermal fluid pH at different Locations
(Source: Researcher, 2019)

The trend exhibited by the pH as illustrated in figure 4.1 is characterized by a significant decrease between sampling point 1 to 2 and a slight increase between point 2 and 3. The significant drop between 1 and 2 is because, during separation most of the liquid phase being separated is brine which is basically sodium chloride solution with high pH value. The resultant steam is drier and more acidic as compared with the original fluid from the production well.

The trend between sampling point 2 and 3 is characterized by an increase. This is because inside the turbine chamber, highly acidic and corrosive elements like chloride and sulphide ions react with other elements such as iron and silica to form solid compounds hence affecting the fluid pH. Also at point 3, water is introduced through spray jets into the condenser to condense the steam to hot water. Usually, the water introduced is from the cooling tower which is treated with biocide and calcium carbonate to control the development/growth of micro-organic matter and pH respectively.

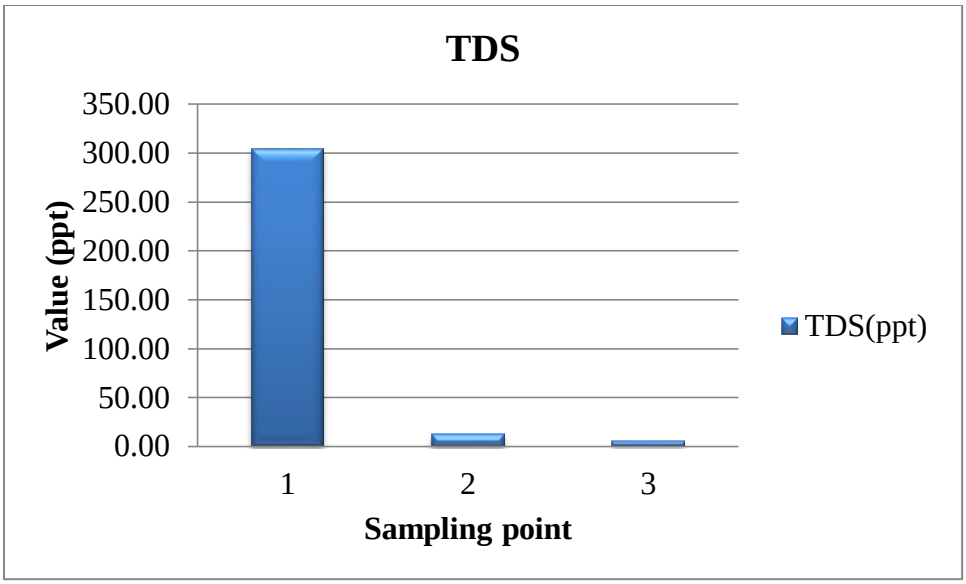

Figure 4. 2: TDS Quantity at sampling points
(Source: Researcher, 2019)

The trend exhibited by TDS Quantity is characterized by a continuous decrease as illustrated in figure 4.2. However, between sampling point 1 and 2, the drastic decrease is due to the separation within the separator where most of it is eliminated together with the brine. Further reduction between point 2 and 3 is due to chemical interactions within the turbine steam chamber leading to formation of solid compounds which are deposited on the turbine parts. As the steam passes through the turbine, it is condensed as the temperature reduces and compounds soluble only at high temperatures solidifies in different configurations forming complex compounds. This explains the reduction in the quantity of TDS in the geothermal fluid downstream of the turbine but a resultant deposition of solids on the turbine parts.

On the other hand, Conductivity highly depends on the quantity of ions present in the fluid. The trend exhibited by conductivity as a parameter in characterization of geothermal fluid for subject power plants, is illustrated in figure 4.3. The drastic reduction in conductivity between sampling point 1 and 2 is as a result of reduced quantity of ions caused by the geothermal fluid separation. Further reduction between

point 2 and 3 is due to chemical reactions within the turbine chamber forming compounds which are deposited on the equipment surfaces as solids.

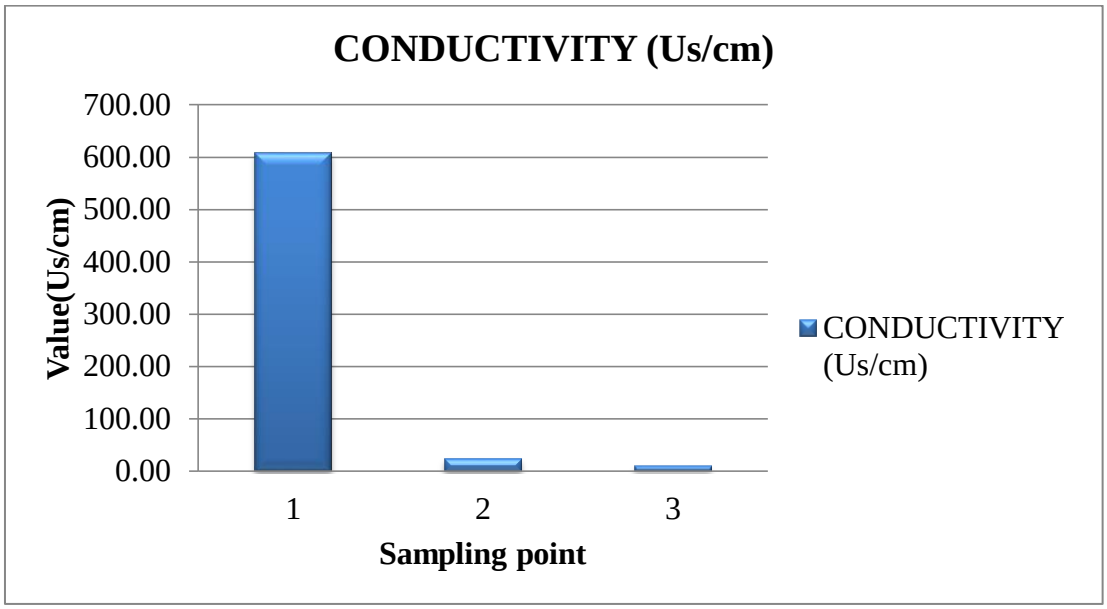

Figure 4. 3: Conductivity Values at different sampling points
(Source: Researcher, 2019)

Both Chloride and Sulphate ions are the most aggressive ions found in the geothermal fluids. Their presence has a huge impact on the geothermal equipment as they are highly corrosive. These ions combine with hydrogen ions from condensed steam to form acidic solutions in form of hydrochloric and sulphuric acids respectively. At high temperatures such as the turbine's operating design temperatures for the well head plants ranging from 190 - 210^{o}C with corresponding pressures of 12.5 – 13.5 bars, these ions react with the turbines' parent material mainly iron (Fe^{2+}) to form chloride and Sulphate compounds. They also combine with other steam constituents such as silicon and sodium to form complex compounds of silica such as Danalite and Halite. These compounds are deposited on the turbine parts as solids. Therefore, they contribute to corrosion as well as deposition/scaling in the turbines.

The trend exhibited by both chloride and Sulphate ions are characterized by continuous reduction as illustrated by figures 4.4 and 4.5. The drastic reduction between sampling

points 1 and 2 is as a result of separation where both are separated in the form of chlorides and Sulphate solutions respectively.

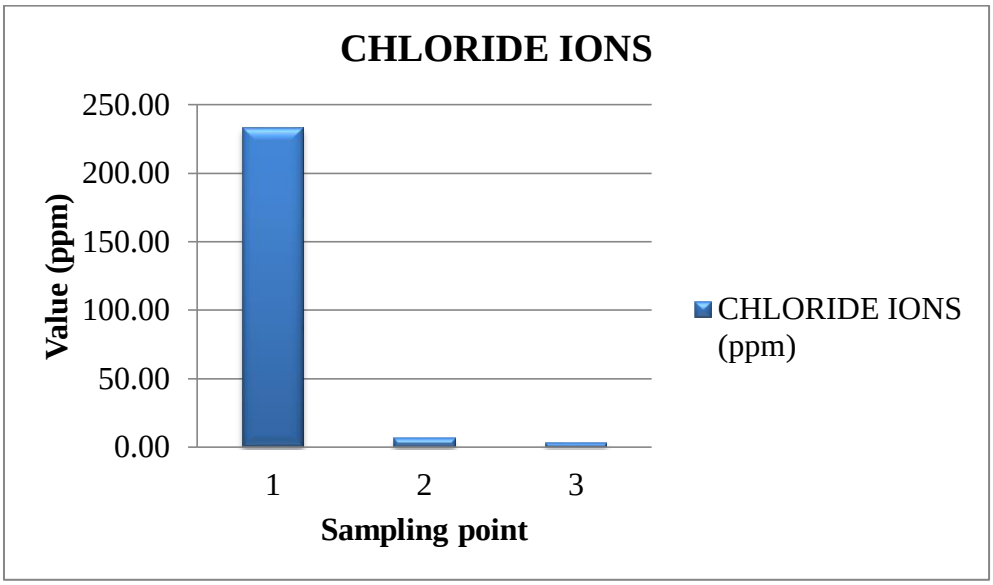

Figure 4. 4: Quantity of chloride ions at different sampling points
(Source: Researcher, 2019)

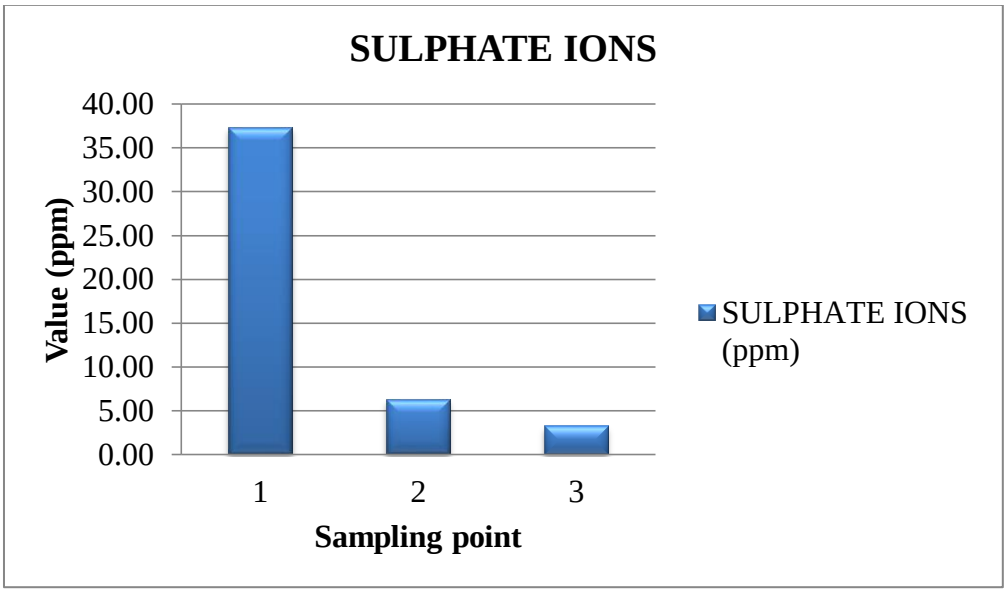

Figure 4. 5: Quantity of Sulphate ions at different sampling points
(Source: Researcher, 2019)

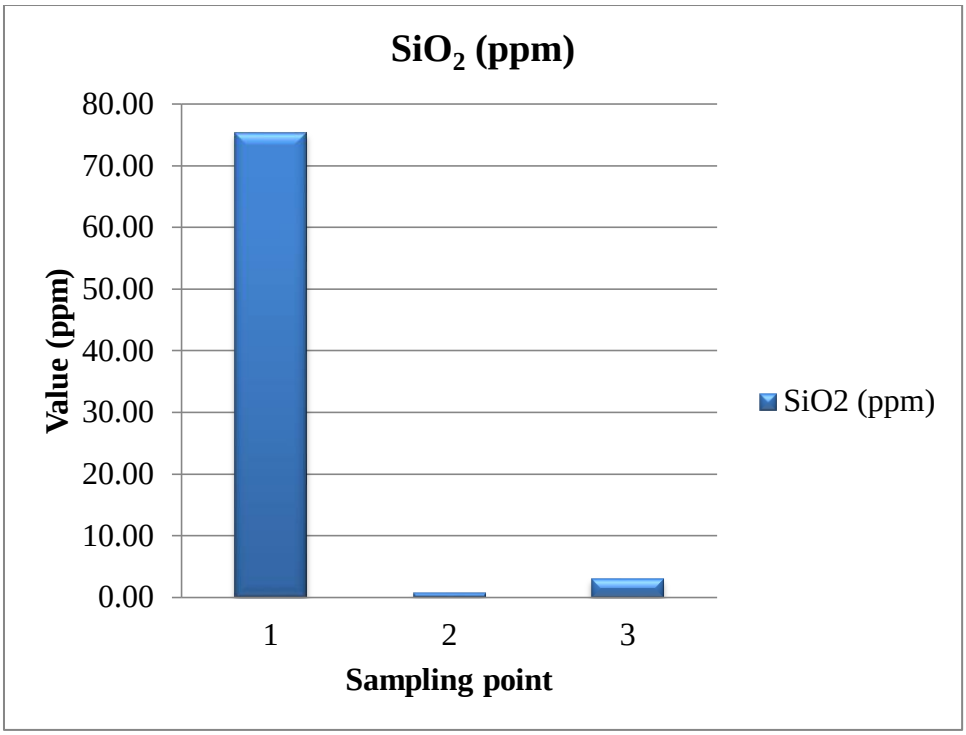

Figure 4. 6: Quantity of SiO_2 at different sampling points
(Source: Researcher, 2019)

As the geothermal fluid is naturally being produced from the production well it is accompanied by silica compounds in different configurations which are basically the complex compounds of silica. However, its abundant configuration is in the form of Quartz, SiO_2 which is soluble in steam at very high temperatures. As the geothermal fluid is purified at the separator, most of the silica compounds combined with the liquid phase which is mostly brine is eliminated and as it is being discharged as geothermal condensate, they solidify forming extremely hard solid material visible on the surfaces of installed equipment. This therefore explains the high decrease in the observed quantity between the sampling points 1 and 2 as illustrated in figure 4.6.

The steam Turbine for the well head plants, are designed to operate between 12.5 - 13.5 bars with corresponding temperatures between 190 to 210^{o}C. This range corresponds to the temperature at which silica changes its state into solid. Below 197^{o}C silica solidifies also in different configurations based on the composition of the geothermal

fluid and conditions favoring its interaction with other elements; hence formation of the solid complex compounds deposited in the surfaces of the equipment.

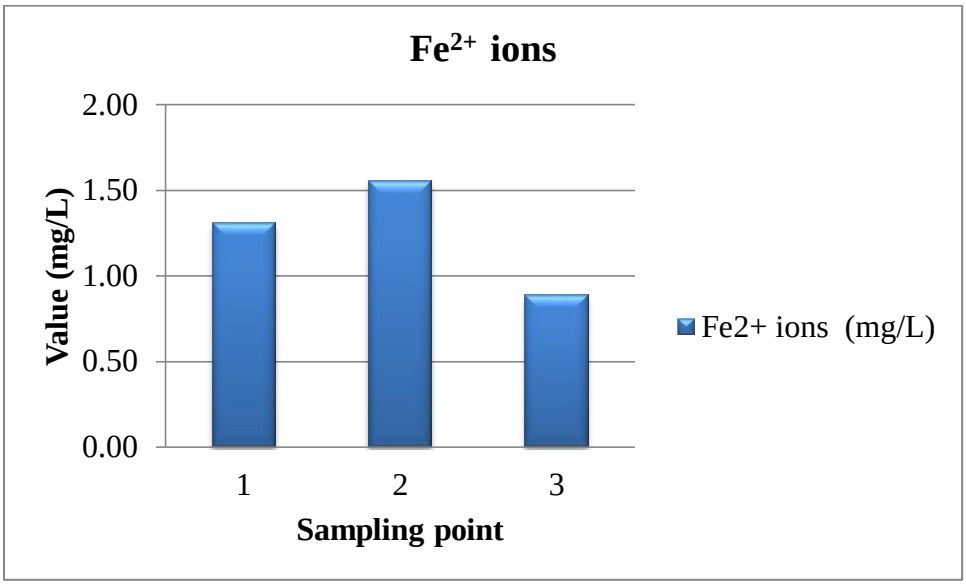

Figure 4. 7: Quantity of Fe^{2+} ions at different sampling points
(Source: Researcher, 2019)

Iron naturally occurs within the earths' crust as an ore. Its existence in the geothermal fluid is as a result of the combination of both dissolved naturally occurring and corroded iron material from the production well piping and equipment installations; hence the significant quantity as indicated in figure 4.7.

All the installations after the production well throughout the hot side of the power plant is made up of carbon steel material which is highly rich in iron. The separator being one of the major installed pressure equipment always containing large volumes of water and condensate is vulnerable to high levels of corrosion and erosion through rusting and abrasion. This explains the reason for the increasing trend in the quantities observed between sampling point 1 and 2 as illustrated in the figure.

Inside the turbine steam chamber, operating conditions are favorable for iron to react with other elements and compounds such as chloride and Sulphur ions to form chlorides

and sulphides, as well as combining with silica to form complex solid compounds such as Danalite and Mitridatite; hence the reduction in the quantity of iron cation as observed in the trend illustrated in figure 4.7.

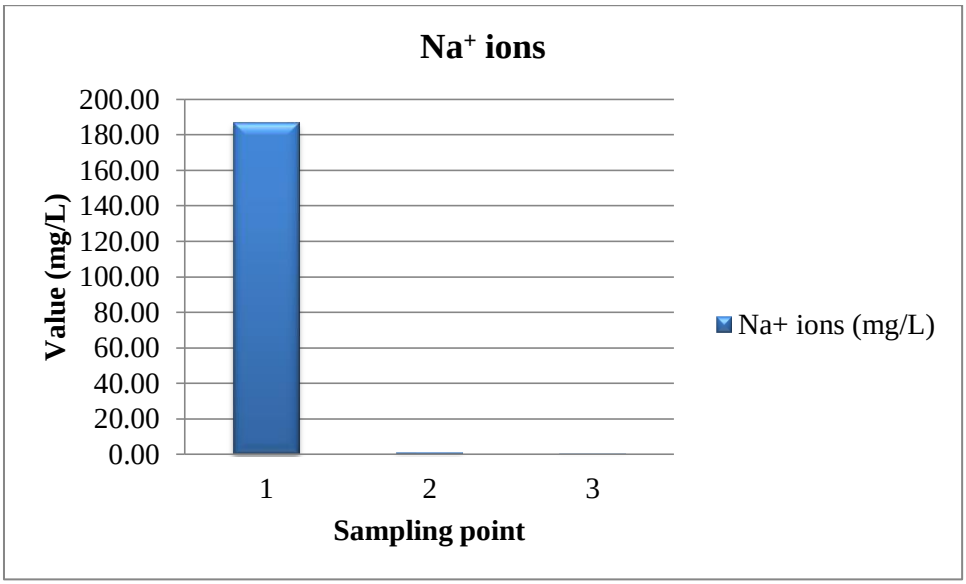

Figure 4. 8: Quantity of Na^+ ions at different sampling points
(Source: Researcher, 2019)

Sodium is a highly reactive element. It easily combines with chloride ions to form sodium chloride solution which is highly basic. The solution produced from the combination is normally referred to as brine. The trend exhibited by the sodium ions in the geothermal fluid is illustrated in figure 4.8. Most of it is eliminated from the fluid at the purification or the separation stage as it makes up all the condensate discharged as brine from the separator. Only negligible traces are found at sampling points 2 and 3 of the geothermal fluid system; hence the trend as observed.

4.2 Characterization of Solid Deposits

The analyses of solid deposits collected from the turbine parts were done using two methods in order to determine their composition. These methods include:

- X-Ray Diffraction (XRD analysis) – was employed to quantitatively analyze the compounds present in the scales/deposited materials. The results were presented as shown in section 4.2.1.
- X-Ray Florescence (XRF analysis) – was used to analyze the elemental composition of deposited materials; the results for the analysis were presented in section 4.2.2

4.2.1 X-Ray Diffraction (XRD) Analysis

The procedure for carrying out XRD analysis is detailed in section 2.7.1. An XRD analyzer employs an X-ray beam with an angular configuration to the surface of the sample to identify the compounds present in the sample based on the atomic arrangement and configurations on the surface of the samples. The analyzer is able to produce the quantitative composition of compounds present in the samples.

In this study, two samples of solid deposits were analyzed by XRD. The sample identification and reference were numbered as 4922/19 and 4923/19. The results were presented in Tables 4.2 and 4.3 respectively. S-Q column indicates the percentage composition of the compounds which were then presented using pie charts as indicated in the figures 4.10 and 4.12;

Table 4. 2: XRD Report for Solid sample No. 4922/19

Index	Compound Name	Formula	Pattern #	I/Ic DB	S-Q
2	Cuprite	Cu2 O	COD 9005769	11.020	2.1 %
4	Danalite	Be3 Fe4 O12 S Si3	COD 9000953	5.170	51.8 %
5	Mitridatite	Ca2 Fe3 H6 O17 P3	COD 9012505	2.910	3.1 %
1	Quartz	O2 Si	COD 9010144	2.990	42.5 %
3	Tungsten	W	COD 9006511	41.890	0.5 %

(Source: Researcher, 2019)

Table 4. 3: XRD Report for Solid sample No. 4923/19

Index	Compound Name	Formula	Pattern #	I/Ic DB	S-Q
2	Halite	Cl Na	COD 9008678	5.020	22.6 %
1	Quartz low	O2 Si	COD 1011159	4.820	77.4 %

(Source: Researcher, 2019)

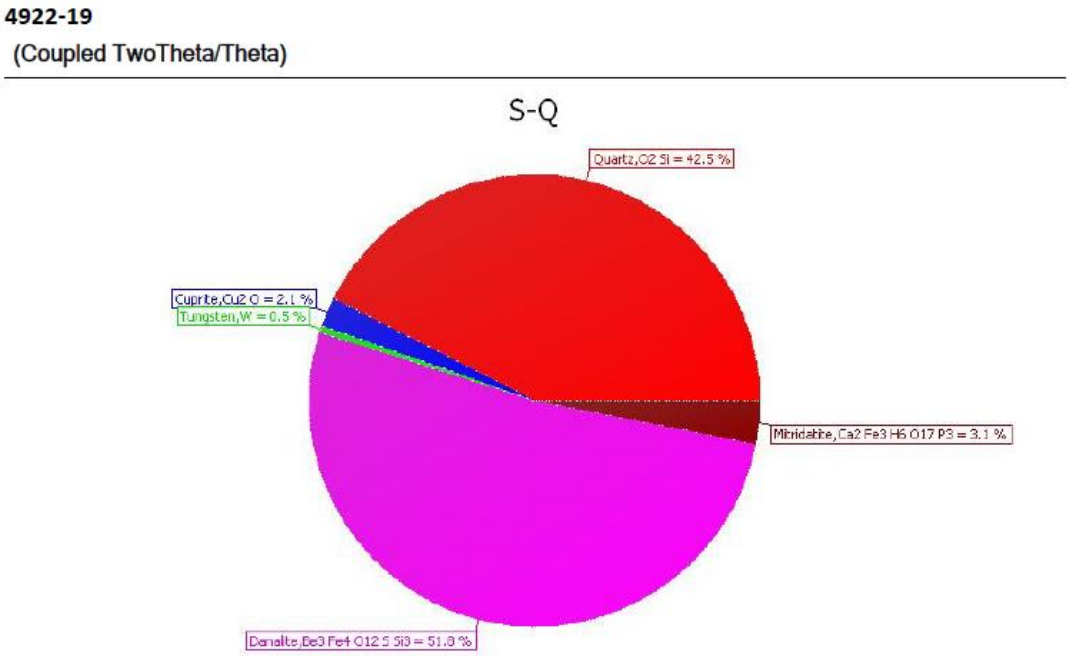

Figure 4. 9: Percentage composition of Compounds present in sample 4922/19
(Source: Researcher, 2019)

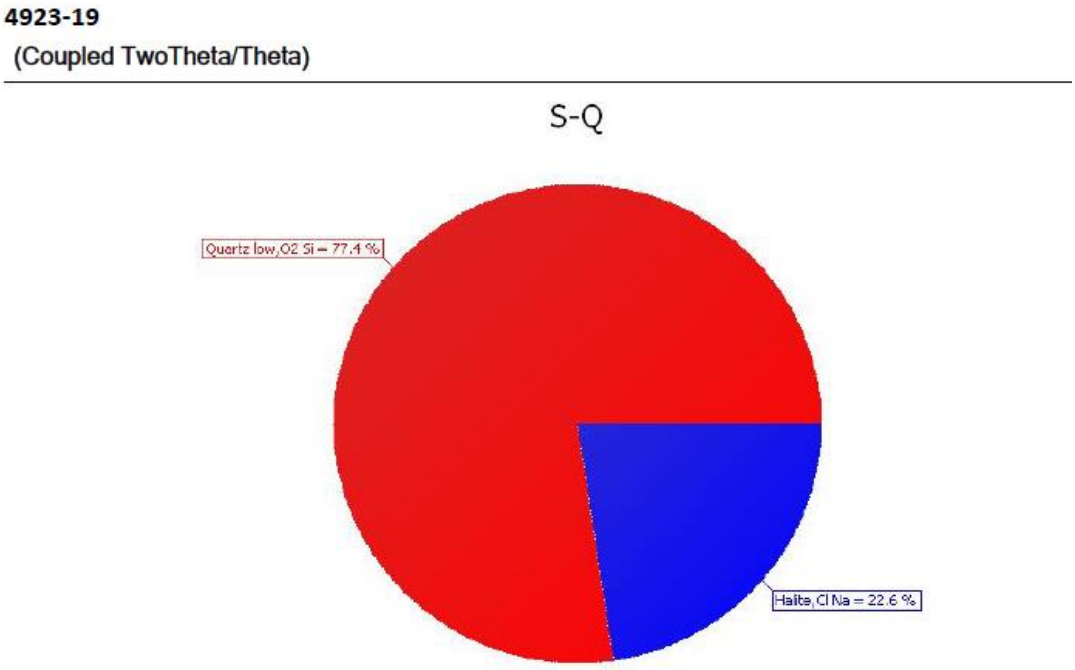

Figure 4. 10: Percentage composition of Compounds present in sample 4923/19
(Source: Researcher, 2019)

As a compound is identified on the face of the sample based on atomic configuration and intensity, a peak signal is shown on the screen of the analyzer and a color is assigned to it. Each element is assigned a specific color code and each time it is recognized a signal is shown. Finally, the analyzer sums up all the peaks for every compound and generates a percentage composition report as tabulated in the tables. The peak signal configurations are as indicated in the figures 4.9 and 4.10.

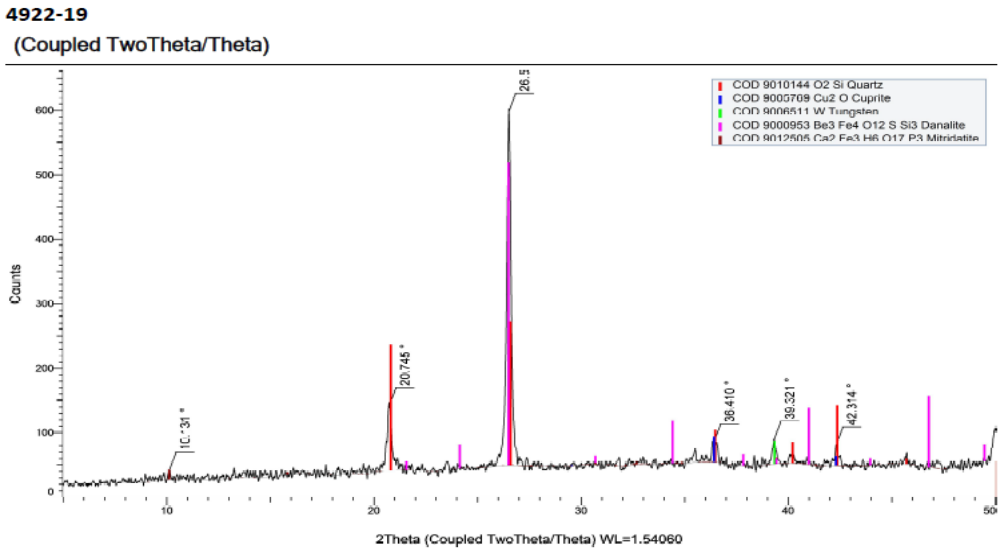

Figure 4. 11: Peak Signal Configuration for Sample 4922/19
(Source: Researcher, 2019)

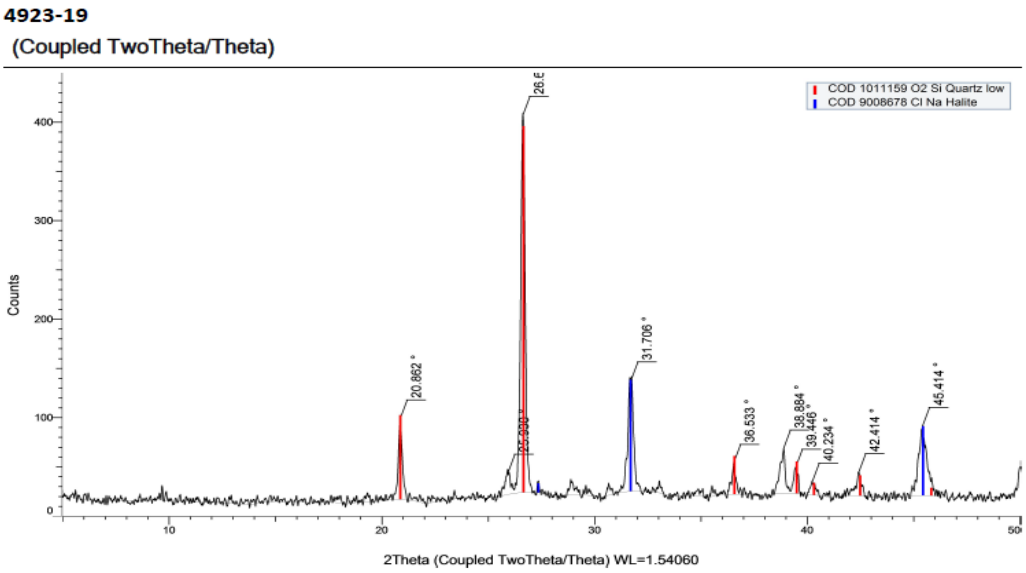

Figure 4. 12: Peak Signal Configuration for Sample 4923/19
(Source: Researcher, 2019)

4.2.2 X–Ray Florescence (XRF) Analysis

XRD analysis is only limited to quantification of compounds present in the samples. For the study, it was necessary to carry out the elemental analysis to ascertain the chemical composition of the solid deposits. By doing so, it aided in comparing the composition of geothermal fluid to that of the deposits so as to confirm the root cause

of the subject defects in the turbine; hence X-Ray florescence (XRF) analysis were carried out for the same samples and the results presented in the table 4.4;

Table 4. 4: XRF analysis report for the solid samples

SOLID DEPOSITS' ANALYSIS REPORT												
ANALYSIS METHOD: X-RAY FLORESCENCE (XRF)												
	% composition											
SAMPLE ID	Fe	K2O	SiO2	Mn	P2O5	S	Cl	Ca	Cr	Ti	Ba	
4922/19 (KWG 6)	20.51	1.99	71.09	0.43	1.54	1.05	0.11	1.27	0.22	0.31	1.06	100
4923/19 (KWG 2)	7.05	16.17	61.31	0.81	1.83	5.74	4.84	1.19	0.16	0.46	0.34	100
MEAN	13.78	9.08	66.20	0.62	1.69	3.40	2.48	1.23	0.19	0.39	0.70	100

(Source: Researcher, 2019)

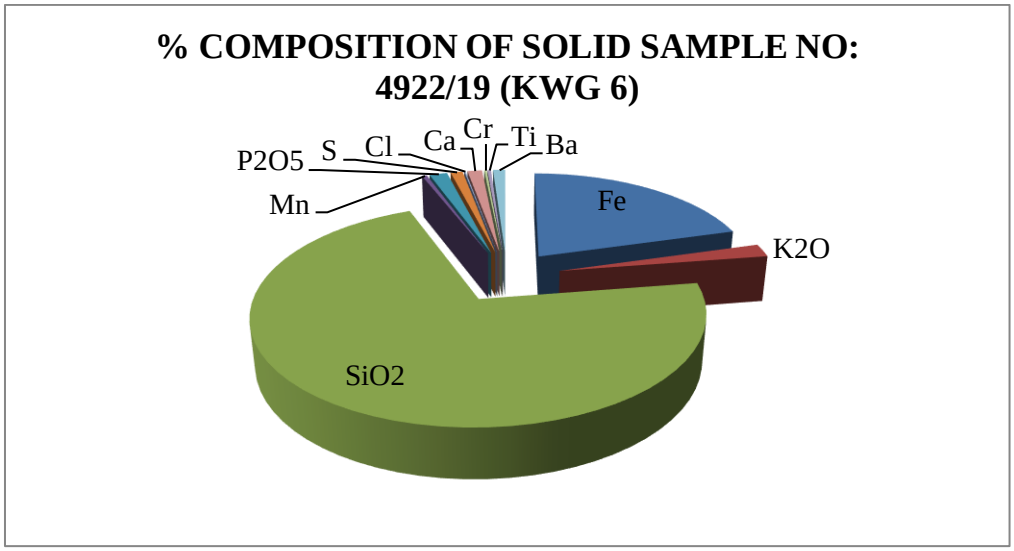

Figure 4. 13: % Composition of solid sample No. 4922/19
(Source: Researcher, 2019)

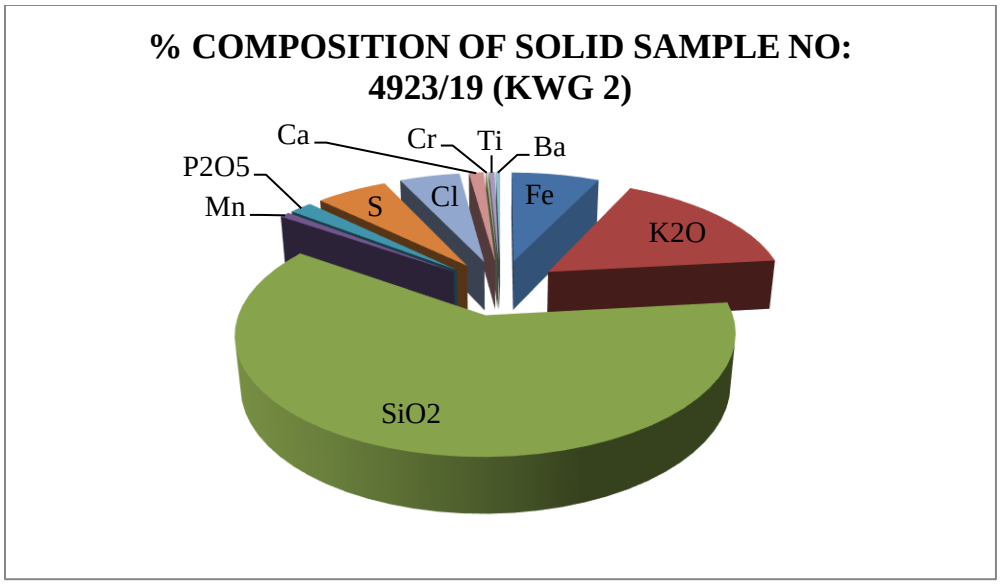

Figure 4. 14: % Composition of solid sample No. 4923/19
(Source: Researcher, 2019)

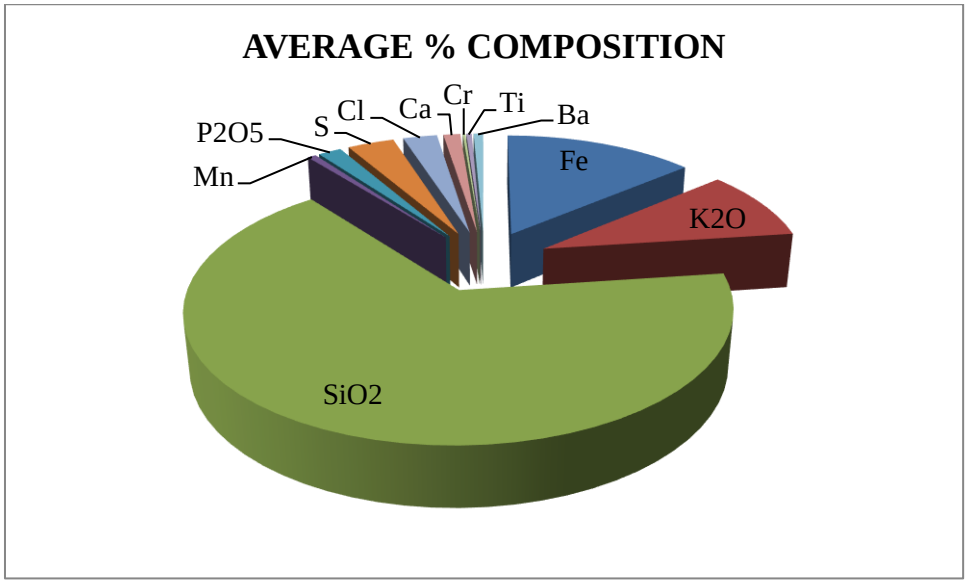

Figure 4. 15: Average % Composition of the solid samples
(Source: Researcher, 2019)

The analysis shows that silica in form of SiO_2 is the largest composition of the solid deposits followed by iron Fe, K_2O, Sulphur, chlorides, P_2O_5 Calcium, Manganese and finally small percentages of Chromium, titanium and Barium. All these elements and compounds originate from the geothermal steam. Their formation details are covered in the discussions from Section 4.1.

In order to ascertain the impacts of geothermal fluid composition on the turbine set being the source of impurities that contributes to corrosion/erosion and deposition/scaling, a turbine blade from one of the failed turbine was sampled and analyzed. The focus of this analysis was to determine the chemical composition of the parent material and evaluated whether the material selected was suitable for the application based on its strength and resistance to erosion/corrosion. The results for the analysis were as presented in Section 4.3.

4.3 Analysis of Turbine Blade Sample

For this study, two methods were selected to carry out the analysis of the blade sample. These are:

a) **Metal Scan (using Metal Scanning Spectrometer)** - was used to analyze a turbine blade sample to determine the elemental composition of the parent material.

In this method, the full blade sample was analyzed in a spectrometer. The largest surface of the sample was polished to ensure that no impurities were present so as not to alter the result. The spectrometer uses a heat spectrum in the identification of the elements present in the sample. Depending on the heat dissipated by each element in the composition, a probe picks up the heat signal on the opposite surface and translates as an element making up the composition. Three test runs were carried out and an average done as the representative of the actual composition. The results of the analysis were presented as shown in the table 4.5 and figure 4.16.

Table 4. 5: Composition of Turbine blade sample

TURBINE BLADE ELEMENTAL ANALYSIS REPORT											
ANALYSIS METHOD: METAL SCAN SPECTROMETER											
	% composition of Elements										
Test run	**Fe**	**C**	**Si**	**Mn**	**Cr**	**Mo**	**Ni**	**Co**	**V**	**W**	
1	85.26	0.03	0.453	0.613	12.4	0.4	0.555	0.04	0.0916	0.244	100
2	84.56	0.03	0.781	0.568	12.8	0.4	0.552	0.04	0.0906	0.214	100
3	85.01	0.03	0.676	0.552	12.5	0.4	0.548	0.04	0.0907	0.242	100
MEAN	84.94	0.03	0.64	0.58	12.57	0.40	0.55	0.04	0.09	0.23	100

(Source: Researcher, 2019)

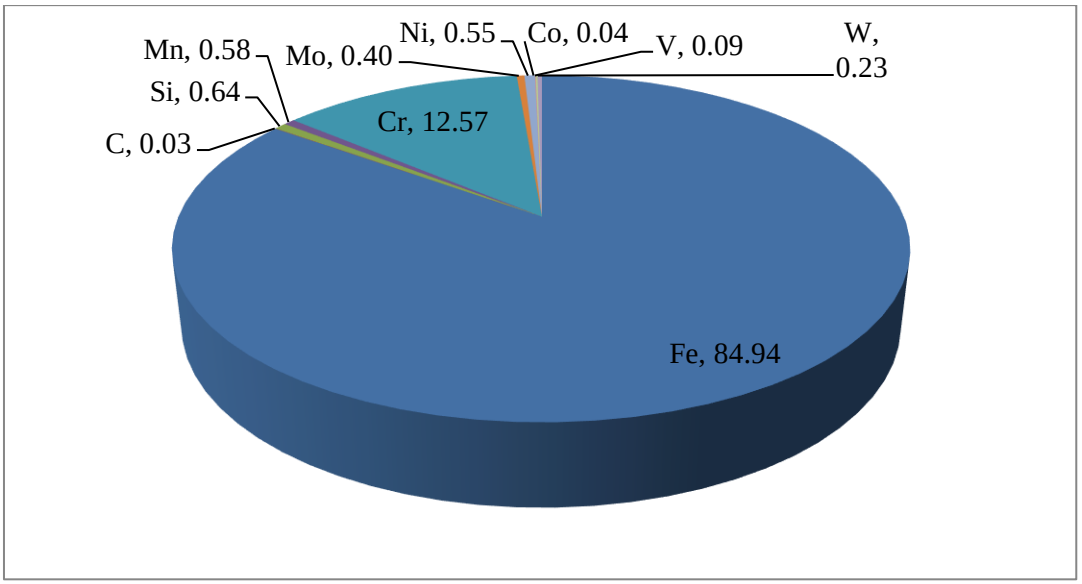

Figure 4. 16: Representation of Turbine blade analysis
(Source: Researcher, 2019)

b) X-Ray Florescence (XRF analysis) – was used to analyze the elemental composition of metal chippings from the turbine blade sample;

For this method the sample was drilled in four different points to produce metal chippings. All the chippings were mixed together into one homogeneous sample as a representative of the whole sample material. The chippings were then fed in to an XRF analyzer and the results were obtained as presented in table 4.6 and figure 4.17.

Table 4. 6: XRF analysis report for blade sample

TURBINE BLADE ELEMENTAL ANALYSIS REPORT											
ANALYSIS METHOD: X-RAY FLOURESCENCE (XRF)											
	% composition of Elements										
Test run	Fe	P	Si	Mn	Cr	Al	Ni	Cu	S	W	
	82.64	0.59	0.81	1.17	12.53	0.16	0.818	0.14	0.77	0.059	100

(Source: Researcher, 2019)

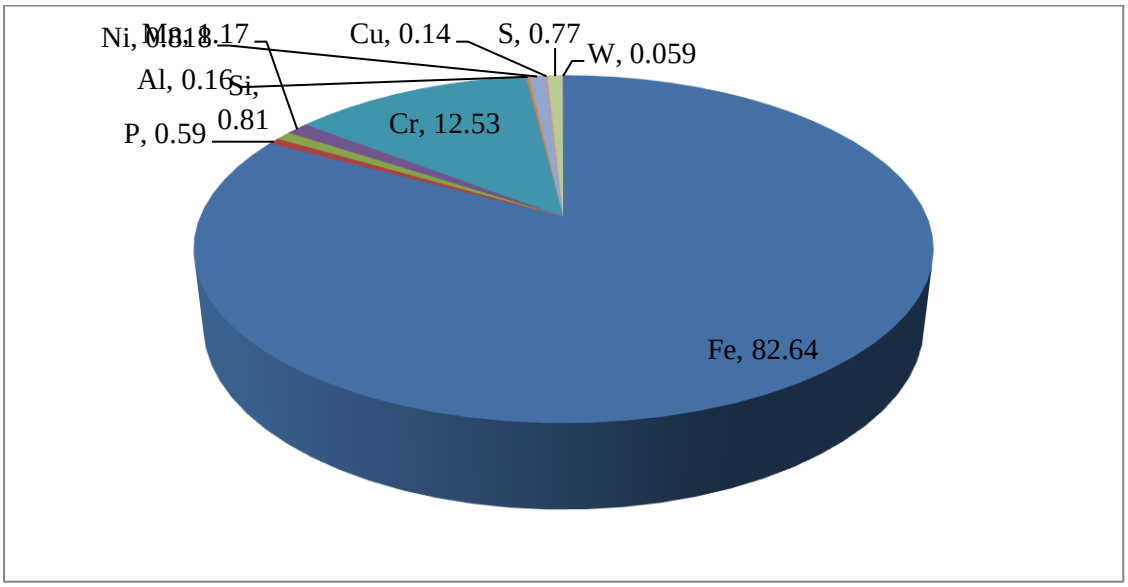

Figure 4. 17: Representation of XRF report for Blade Composition
(Source: Researcher, 2019)

From the analysis, the results characterizes the parent material as an alloy steel with the highest composition being iron Fe, and an average chromium content of 12.5%. Chromium is an important element in alloy steels as it increases the hardenability while ductility is not affected. High chromium content increases steel corrosion resistance, tensile strength and yield strength. Chromium- Nickel combination ensures good tough hardening, heat resistance and resistance to scaling.

4.4 Causes of the defects Observed in the Turbines at WHP Plants

Material selection is an important consideration in the design of a geothermal turbine. In the process, it is also important to look in to the operating conditions of the turbine

and the environment in which it operates. Olkaria's geothermal plants were designed to operate with the parameters indicated in table 4.7.

Table 4. 7: Design parameters for Olkaria's Geothermal Power Plants

	Turbine inlet Pressure (bars)	**RPM**	**Turbine Temp (^oC)**
Conventional plants	5.0	3000	151
Wellhead Plants	13.5	6000	191

(Source: Design and O&M manuals, 2010)

The data shown it table 4.7 indicates that the conditions under which the well head plants are subjected to during operation are more harsh and aggressive as compared to the conventional plants. This therefore means that the selected material should be stronger for well head plant's turbines as compared to that of conventional plants.

In the existing conventional geothermal power plants, 16% Cr, chromium steel material has been used in the manufacturing of the turbine blades (MHPS, 2010). Their performance has been quite successful as the first installed turbines have operated for 35 years without any observed failure. The results obtained in this research indicates that the material selected for the well head power plants is made up of 12.5% Cr, chromium steel which is relatively low as compared with the recommended 16%Cr 4%Ni for the conventional plants. This therefore means that the strength and its resistance to corrosion are lower for the well head turbine blades. This can be related to the defects observed in the well head turbines while there is hardly any observed from the conventional plants.

Considering the composition of the geothermal fluid for the well head plants, site conditions should have been the critical requirement during the design stage to ensure that the selected material is of the right quality in terms of strength and resistivity to corrosion. However this could have been missed out leading to the selection of a weaker material with low resistance to corrosion as indicated by the research findings. In summary, the research attributed the root cause of the observed defects to;

- Steam quality
- Blade material's resistance to corrosion

4.5 Methods of Eliminating Scaling/Deposition And Erosion/Corrosion

During the research process, it was found that the corrosive nature of the geothermal fluid have got an adverse effect on the turbines. It is for this reason that turbine manufacturers in their quest to enhance their turbine efficiencies and reliability developed technologies to counter cases of erosion/corrosion. In order to remedy the defects, a review of various design manufacturing considerations and recommendations were carried out as detailed in section 2.9.

From the review, the three described technologies informed the basis at which the affected turbine was refurbished. Despite the fact that all of them were relevant to design and manufacturing stages and not applicable at the time in which the defects were observed, they could be emulated and adopted during repair and maintenance of the subject turbine. Surface cleaning and repairs were required to recondition the turbine to its original state. However, the methodology used had to comply with the manufacturing standards and procedures to ensure that the repaired turbine was fit for purpose and that it poses no risk of damage or loss bearing in mind that it is a high precision equipment operating at very high speed and sensitive conditions. It was for

this reason therefore that hard facing and machining techniques were determined as suitable methods of eliminating the defects on the affected turbine.

4.6 Performance Enhancement for the Turbines

Following a successful implementation of the hard facing and machining techniques on an affected turbine as described in section 3.6, positive results were observed on its performance. Internal leakages, chocking of steam paths and rough surfaces were eliminated. The efficacy of these repairs was the restoration of plant performance to an impeccable prominence. Distortion and erosion correction on diaphragms along with repairs on steam gouged surfaces turn the struggling plant to a formidable power plant. The refurbishment resulted in improving the turbine's output from 2.75 MW to its design rated output of 3.20 MW while maintaining low rotor vibrations with normal bearing temperatures among other parameters. Considering the same quantity of steam being consumed, the energy conversion efficiency was increased by 16.4%; hence, the turbine performance was enhanced.

CHAPTER FIVE

CONCLUSIONS AND RECOMMENDATIONS

5.1 Conclusions

Analysis of the geothermal fluids at various sections of the plants indicated the characteristics of the geothermal fluids in terms of pH, TDS, Conductivity, chloride ions, Sulphate, silica and Cations mainly Iron and Sodium. The composition of steam as it enters the turbine chamber, the design conditions of the turbines, the characterization of the scales/deposits samples at the turbines, composition of the turbine blade sample as well as the steam compositions at the turbine's exhaust were of significance in establishing the conditions favoring defects formation in the turbine.

According to the research findings, it was concluded that the root cause of the subject defects observed in the well head plants are:

1. Low material resistance to corrosion – this was confirmed by the low chromium content of 12.5% Cr, for the material used to manufacture the turbine blades. Considering the conventional turbine blades which were manufactured with higher percentage chromium steel of 16% Cr, in relation to it operating conditions (5.0 bars, 3000 rpm and 151 ^{O}C), the material for well head plants ought to have been stronger basically with a higher percentage of chromium in order to sustain the harsh operating conditions of 13.5 bars, 6000 rpm and 191 ^{O}C.
2. Geothermal fluid/steam quality – The pH value, chloride and sulphate ions in the fluid signify acidity and its highly corrosive nature. Significant amounts of oxides in deposits indicate oxidation reactions as the fluid interacts with the metals at elevated temperatures leading to deposition/scaling. It also shows

that there is quite a significant amount of moisture carry over which finds its way in to the turbine steam chambers playing a major role as an oxidizing agent and providing favorable conditions for corrosion.

Upon the clear understanding of the root cause of the defects on the turbines, suitable repair techniques were required to reinstate the turbine in to good working condition and it was for this reason that hard facing and machining methods were determined and implemented. Their implementation of these resulted in a significant improvement of the turbines output from 2.75 MW to its design rated output of 3.2 MW. This is equivalent 16.4% enhancement of the turbine's performance.

5.2 Recommendations

The research has identified the root cause of the subject defects being the turbine blade's material having low resistance to corrosion and geothermal fluid/steam quality. This facilitated the determination of hard facing and machining techniques as suitable methods of eliminating the defects and their implementation on an affected turbine which resulted in increased output from 2.75 MW to 3.20 MW. The research therefore recommends the following;

1. Further studies need to be carried out to investigate the impacts of hard facing and machining techniques on the life span of the turbine.
2. Proper feasibility studies need to be carried out prior to turbine design and manufacturing to ensure that suitable material is selected based on the conditions it's expected to operate under.
3. Further studies should be done to determine ways of improving steam quality upstream of the turbine so as to prevent the defect formation in the turbine sets.

4. Reduced time interval between maintenance cycles to ensure that the defects are detected early and addressed before attaining critical stages causing serious impacts on the turbines.

REFERENCES

Ahned M & Sürken N. (2009) Experimental assessment of droplet impact erosion resistance of steam turbine blade materials *Wear* 267(9-10**)** 1605-1618

Amjad, Z. (2010). The Science and Technology of Industrial Water Treatment, Boca Raton, Florida: *Taylor & Francis Group*, LLC.

Arnorsson, S. & Stefansson, A. (2007), Fluid-fluid interactions in geothermal systems. *Rev Mineral Geochem* 65 (1) 259-312.

Arnórsson, S. & Olafsson (2007) Deposition of calcium carbonates minerals from geothermal waters – theoretical considerations. *Geothermics, 18,* 33-39.

Arnórsson, S., Angcoy, Jr., E.C., Bjarnason, J.Ö., Giroud, N., Gunnarsson, I., Kaasalainen, H., Karingithi, C., and Stefánsson, A., (2010). Gas chemistry of volcanic geothermal systems. *Proceedings World Geothermal Congress, Bali, Indonesia.*

Ashree Technical Committee (2002), *Geothermal Energy Working Draft*, Atlanta: Tullie Circle NE.

Axelsson, G., & Gunnlaugsson, E., (2000). Long-term monitoring of high-and low-enthalpy fields under exploitation, *World Geothermal Congress 2000, pre-congress course, Kokonoe, Japan.*

Bergna, H. E. & Roberts, W. O. (Eds.) (2006). Colloidal silica: Fundamentals and applications. Boca Raton, FL: Taylor & Francis Group.

Brown, K. (2011). Thermodynamics and kinetics of silica scaling, *International Workshop on Mineral Scaling*, Manila

Cuevas-Artega C, Rodriguez J A, Clemente C M & Rodríguez J M (2014). Pitting Corrosion Damage for Prediction Useful Life of Geothermal Turbine Blade *American Journal of Mechanical Engineering* 2(6) 164-168.

Criaud, A., and Fouillac, C., (1989). Sulfide scaling in low-enthalpy geothermal environments: a review. *Geothermics,* 18, 73-81.

DiPippo R. (2008). Geothermal power plants: principles, applications, case studies and environmental impact: *Elsevier.* 8(1) 43-51.

Duthie, R.G. and Nawaz, M. (1989). Comparison of direct contact and kettle reboilers to reduce non-condensables in geothermal steam', *Transactions Geothermal Resources Council*, 13(1) 575–580.

Giroud, N. (2008). *A chemical study of arsenic, boron and gases in high-temperature geothermal fluids in Iceland, Doctoral dissertation, Dissertation for the Degree of Doctor of Philosophy,* University of Iceland.

Gunnarsson, I., Arnórsson, S., & Jakobsson, S. (2005). Precipitation of poorly crystalline antigorite under hydrothermal conditions: *Geochim, Cosmochim. Acta,* 69(1) 2813-2828.

Karingithi, C. W., Arnórsson, S., and Gronvold, K., 2010: Processes controlling aquifer fluid compositions in the Olkaria geothermal system, Kenya. *Journal of Volcanology Geothermal Resource* 196 (1) 57-76.

Khalifa, H.E. & Michaelides, E., (1978). *The Effect of Noncondensable Gases on the Performance of Geothermal Steam Power Systems*, US Department of Energy, Report No. CATMEC/28: Rhode Island, USA.

Kristmannsdóttir, H., Sigurgeirsson, M., Ármannsson, H., Hjartarsson, H., and Ólafsson, M., (2000). Sulphur gas emissions from geothermal power plants in Iceland. *Geothermics, 29*, 525-538.

Malimo, S. J. (2013). Fluid Chemistry of Menengai Geothermal Wells, Kenya, *Geothermal Resources Council Transactions,* 37(1) 56-62.

Meier, M (2001). *User's Manual Scintag XDS 2000 X-Ray Diffractometer PCDMS Version*. Materials Science Central Facilities Department of Chemical Engineering and Materials Science University of California, Davis.

Montero, G. (1990) 'Evaluation of the network of a turbine operated by a mixture of steam and non-condensable gases', *Proceedings of 12th New Zealand Geothermal Workshop*, 11(1) 163–174.

Omenda, P. A.: (2000) Anatectic origin for comendite in Olkaria geothermal field, Kenya Rift; Geochemical evidence for syenitic protholith, *African Journal of Science and Technology. Science and Engineering series*: 1, 39-47.

Ormat, (2001). The power of innovation, projects, geothermal power plants*: Ethiopia, Aluto-Langano.*

Opondo, K.M. (2008). Fluid Characteristics of the three Exploration wells drilled at Olkaria Domes, Kenya, *Proceedings of the 33rd workshop on Geothermal Reservoir Engineering*, Stanford University, Stanford, Ca, 6pp.

Povarov, P.A., Tomarov, G.V., Semenov V.N. (1997). Russian geothermal resources and problems of metal erosion-corrosion of geothermal power plants: *Proceedings of the World Geothermal Congress. Italy*. 4(1): 2433-2441.

Povarov, O.A., Tomarov, G.V., Zharov, V.N., Kutyrev, C.Yu. (1992). Causes of damages and ways to increase reliability of GeoPP equipment. *Journal. Energeticheskoye Stroitelstvo*, 2(1) 14-20.

Povarov, O.A., Tomarov, G.V., Kutyrev, S. Yu., Velichko, Ye.V. (1991*). Problems of salt depositions and wear of geothermal power unit components*. Moscow: ZniiteiItyazhmash.

Regenspurg S, Wiersberg T, Brandt W, Hueges E. & Saadat A (2010). Geochemical Properties of Saline Geothermal Fluids from the in–Situ Geothermal Laboratory *Chemie der Erde-Geochemistry* 70(3) 101-109.

Sanada, N. Kurata, Y Najo, H.S. Kim, J. Ikeuchi, J. Lichti, K.A (2000). IEA Deep Geothermal Resources Subtask C: Materials Progress with a database for Materials in Deep and Acidic Geothermal Wells. Proceedings Word Geothermal Congress, Kyushu-Tohoku, Japan.

Semenov. N Tomarov, G.V Povarov, N.O & Bezotechestvo, M. L (2002). Formation of deposits in the flow path of turbines at geothermal power stations, Tyazh. Mashinostr., 8(1) 40–45.

Sinclair, L. (2012). *Development of Silica Scaling, Test Rig*: University of Canterbury.

Stefansson A, Arnórsson S, Gunnarsson I, Kaasalainen H. & Gunnlaugsson E. (2011). The geochemistry and sequestration of H_2S into the geothermal system at Hellisheidi, Iceland: *Journal of Volcanology and Geothermal Research* 202(3-4) pp 179-188.

Suwai, J.J. (2011). Preliminary reservoir analysis of Menengai geothermal field exploration wells: *UNU-GTP Publications*, Report 20, 481-509.

Thomas, R (2003). Titanium in the Geothermal Industry. GHC Bulletin, December 2003

Tomarov, G.V. (2012). Erosion-corrosion of structure materials in saturated-steam turbines: *Journal of Teploenergetica*, 7(1) 34-45.

Vorum, M. & Fritzler, E.A., (2000). *Comparative Analysis of Alternative Means for Removing Non-Condensable Gases From Flashed-Steam Geothermal Power Plants*, NREL/ SR-550-28329, National Renewable Energy Laboratory (NREL), Colorado, The USA.

World Energy Council, (2001) *Survey of energy resources.* World Energy Council website:

APPENDICES

Appendix I: Data for Liquid Sample Anaysis

RESEARCH DATA									
LIQUID SAMPLE ANALYSIS									
DATE	SAMPLE II	pH	TDS(p	CONDUCTIVITY (Us/c	CHLORIDE IONS (ppm)	SULPHATE IONS (ppm)	SiO2 (ppm)	IRON (mg/L)	SODIUM ion (mg/L
15/8/2019	1	5.36	600	1200	260	77.8	136.6	0.6	360
	2	4.61	14.8	29.6	4.425	19.15	0.5	4	1.8
	3	4.56	4.26	8.52	4.775	3.3	2.75	0.62	0.8
16/8/2019	1	5.18	250	501	203.841	14.8	62	1.9	145
	2	4.22	10	20	3.375	3.95	0	1.9	0.4
	3	4.71	3.1	6.17	3.975	5.55	0	2.4	0
17/8/2019	1	5.56	255	510	203.8	45.5	62.6	3.7	155
	2	4.92	12.7	25.3	3.85	1.65	0.75	0.62	0.2
	3	5.27	4.33	8.65	2.995	1.65	1.5	0.89	0
18/8/2019	1	5.14	278	556	249.53	21.7	69.3	0.93	180
	2	4.3	20	40	23.92	8.15	1.5	0.83	2.4
	3	4.52	10.5	21.5	0.9	3.2	13.5	0.41	0
21/8/2019	1	5.52	287	573	300.33	36.1	60.9	0.37	144
	2	4.62	10.9	21.8	2.275	3.85	1.5	0.14	0.8
	3	4.86	5.31	10.6	2.425	1.1	0	0.04	0
25/8/2019	1	5.41	155	310	182.11	27.9	61	0.35	138
	2	4.61	6	12	1.7	0.85	0	1.84	0.6
	3	4.82	4.31	8.58	6.025	4.6	0	0.97	0.2

LIQUID SAMPLE ANALYSIS									
SAMPLING POINT 1									
DATE	SAMPLING POINT.	pH	TDS(ppt)	CONDUCTIVITY (Us/cm)	CHLORIDE IONS (ppm)	SULPHATE IONS (ppm)	SiO2 (ppm)	IRON (mg/L)	SODIUM ion (mg/L)
15/8/2019	1	5.36	600	1200	260	77.8	136.6	0.6	360
16/8/2019	1	5.18	250	501	203.841	14.8	62	1.9	145
17/8/2019	1	5.56	255	510	203.8	45.5	62.6	3.7	155
18/8/2019	1	5.14	278	556	249.53	21.7	69.3	0.93	180
21/8/2019	1	5.52	287	573	300.33	36.1	60.9	0.37	144
25/8/2019	1	5.41	155	310	182.11	27.9	61	0.35	138
	MEAN 1	5.36	304.17	608.33	233.27	37.30	75.40	1.31	187.00

LIQUID SAMPLE ANALYSIS									
SAMPLING POINT 2									
DATE	SAMPLING POINT.	pH	TDS(ppt)	CONDUCTIVITY (Us/cm)	CHLORIDE IONS (ppm)	SULPHATE IONS (ppm)	SiO2 (ppm)	IRON (mg/L)	SODIUM ion (mg/L)
15/8/2019	2	4.61	14.8	29.6	4.425	19.15	0.5	4	1.8
16/8/2019	2	4.22	10	20	3.375	3.95	0	1.9	0.4
17/8/2019	2	4.92	12.7	25.3	3.85	1.65	0.75	0.62	0.2
18/8/2019	2	4.3	20	40	23.92	8.15	1.5	0.83	2.4
21/8/2019	2	4.62	10.9	21.8	2.275	3.85	1.5	0.14	0.8
25/8/2019	2	4.61	6	12	1.7	0.85	0	1.84	0.6
	MEAN 2	4.55	12.40	24.78	6.59	6.27	0.71	1.56	1.03

LIQUID SAMPLE ANALYSIS									
SAMPLING POINT 3									
DATE	**SAMPLING POINT.**	**pH**	**TDS(ppt)**	**CONDUCTIVITY (Us/cm)**	**CHLORIDE IONS (ppm)**	**SULPHATE IONS (ppm)**	**SiO2 (ppm)**	**IRON (mg/L)**	**SODIUM ion (mg/L)**
15/8/2019	3	4.56	4.26	8.52	4.775	3.3	2.75	0.62	0.8
16/8/2019	3	4.71	3.1	6.17	3.975	5.55	0	2.4	0
17/8/2019	3	5.27	4.33	8.65	2.995	1.65	1.5	0.89	0
18/8/2019	3	4.52	10.5	21.5	0.9	3.2	13.5	0.41	0
21/8/2019	3	4.86	5.31	10.6	2.425	1.1	0	0.04	0
25/8/2019	3	4.82	4.31	8.58	6.025	4.6	0	0.97	0.2
	MEAN 3	4.79	5.30	10.67	3.52	3.23	2.96	0.89	0.17